Article

Neuron

# Natural and Drug Rewards Engage Distinct Pathways that Converge on Coordinated Hypothalamic and Reward Circuits

## Graphical Abstract

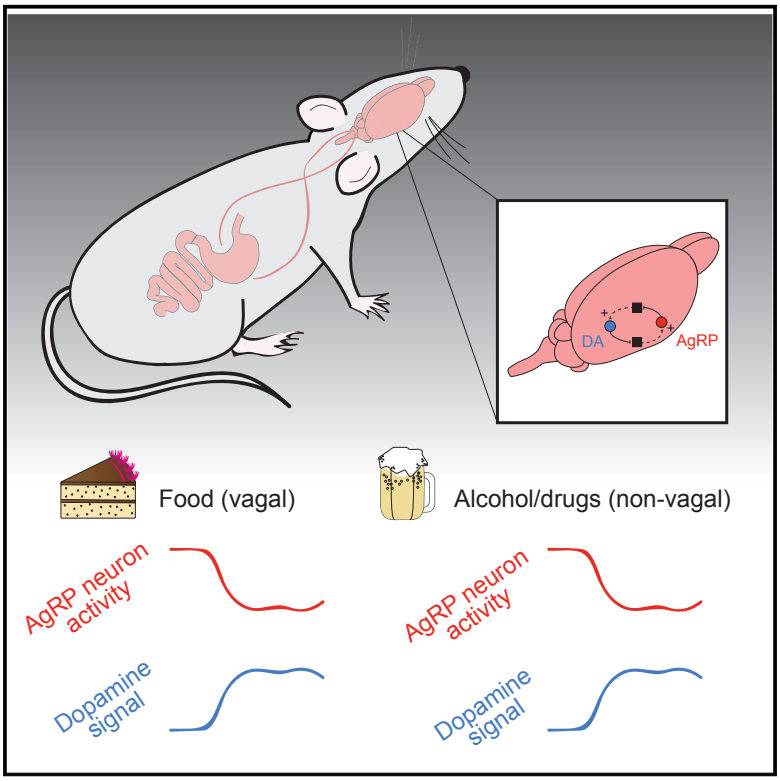


## Authors

Amber L. Alhadeff, Nitsan Goldstein, Onyoo Park, Michelle L. Klima, Alexandra Vargas, J. Nicholas Betley

## Correspondence

jnbetley@sas.upenn.edu

## In Brief

How does the brain process natural versus drug rewards? Alhadeff et al. demonstrate that food and drugs signal from the periphery to the hypothalamus via distinct pathways. Furthermore, bidirectional and coordinated interactions between hypothalamic and dopamine circuits potentiate responses to rewards.

## Highlights

- Alcohol and drugs inhibit hypothalamic neurons in a nutrient-independent manner
- Nutrients and drugs inhibit AgRP neurons via vagal and non-vagal modes, respectively
- Interdependent coordination of AgRP and DA circuits mediates response to rewards

Alhadeff et al., 2019, Neuron *103*, 891–908
September 4, 2019 
https://doi.org/10.1016/j.neuron.2019.05.050

CellPress

Neuron
Article

# Natural and Drug Rewards Engage Distinct Pathways that Converge on Coordinated Hypothalamic and Reward Circuits

Amber L. Alhadeff,[1,2] Nitsan Goldstein,[1,2] Onyoo Park,[1] Michelle L. Klima,[1] Alexandra Vargas,[1] and J. Nicholas Betley[1,3,*]
[1]Department of Biology, University of Pennsylvania, Philadelphia, PA 19104, USA
[2]These authors contributed equally
[3]Lead Contact
*Correspondence: jnbetley@sas.upenn.edu
https://doi.org/10.1016/j.neuron.2019.05.050

## SUMMARY

**Motivated behavior is influenced by neural networks that integrate physiological needs. Here, we describe coordinated regulation of hypothalamic feeding and midbrain reward circuits in awake behaving mice. We find that alcohol and other non-nutritive drugs inhibit activity in hypothalamic feeding neurons. Interestingly, nutrients and drugs utilize different pathways for the inhibition of hypothalamic neuron activity, as alcohol signals hypothalamic neurons in a vagal-independent manner, while fat and satiation signals require the vagus nerve. Concomitantly, nutrients, alcohol, and drugs also increase midbrain dopamine signaling. We provide evidence that these changes are interdependent, as modulation of either hypothalamic neurons or midbrain dopamine signaling influences reward-evoked activity changes in the other population. Taken together, our results demonstrate that (1) food and drugs can engage at least two peripheral→central pathways to influence hypothalamic neuron activity, and (2) hypothalamic and dopamine circuits interact in response to rewards.**

## INTRODUCTION

Motivational drives for natural rewards are mediated by classic homeostatic as well as mesolimbic dopamine (DA) circuits. Increasing evidence demonstrates that homeostatic signals influence reward circuits and behavior, highlighting the importance of research on the complex intersection of these neural circuits and mechanisms (Rossi and Stuber, 2018). The interplay between these systems is supported by the ability of hunger and satiation signals to act on reward circuits to influence feeding behavior (Alhadeff et al., 2012; Dossat et al., 2011; Fulton et al., 2006; Han et al., 2018; Hommel et al., 2006; Kenny, 2011; Liu and Borgland, 2015; Skibicka et al., 2011). But how do rewards influence canonical homeostatic (e.g., hypothalamic) circuits? While the effects of food on hypothalamic circuits are well-characterized (Sternson and Eiselt, 2017), the effects of drugs on the *in vivo* neural activity of hypothalamic neuron populations remain unexplored. As drugs of abuse have been used to reveal reward pathways in the brain (Volkow and Wise, 2005), exploring the effects of these substances on homeostatic neuron populations may provide a better understanding of how these systems interact and are controlled to influence motivated behavior.

From this perspective, alcohol is a particularly interesting drug because it contains calories, has rewarding psychoactive effects, and is thought to influence food intake and body weight. The effects of alcohol on energy homeostasis were first described by Curt Richter in 1941 when he described alcohol as a "food" that can replace other calories as a source of energy (Richter, 1941). This was demonstrated by findings showing that rats decrease food intake in direct proportion to calories obtained from alcohol (Richter, 1953). Although these findings support the homeostatic control of body weight, subsequent studies suggest that alcohol has no effect (Gill et al., 1996) or actually increases (Cains et al., 2017; Hetherington et al., 2001) food intake. In addition to these mixed effects on behavior, the effects of alcohol on *in vivo* neural activity are not fully resolved. While it is known that alcohol increases DA neuron activity (Gessa et al., 1985) and is consumed for its rewarding "drug" properties, it is not clear how alcohol affects *in vivo* activity in hypothalamic circuits that influence motivated feeding behavior.

Agouti-related protein (AgRP)- and pro-opiomelanocortin (POMC)-expressing neurons of the arcuate hypothalamic nucleus are critical to food intake control. AgRP neurons are inhibited and POMC neurons are activated by food intake (Betley et al., 2015; Chen et al., 2015; Mandelblat-Cerf et al., 2015), and stimulating these neuron populations increases or decreases food intake, respectively (Aponte et al., 2011; Krashes et al., 2011). Our recent work demonstrated that calories are necessary for sustained reductions in AgRP neuron activity (Su et al., 2017). Furthermore, nutrients inhibit AgRP neurons in part through the release of gastrointestinal satiation signals (Beutler et al., 2017; Su et al., 2017). It is thought that these signals communicate with the brain through a combination of hormonal action and vagal neurotransmission. Does alcohol use similar mechanisms to influence hypothalamic neuron activity and food intake? A recent study demonstrated that alcohol increases food intake, likely by elevating AgRP neuron activity (Cains et al., 2017).

However, since alcohol contains calories, such a finding is inconsistent with the reported effects of nutrients on *in vivo* AgRP neuron activity. Thus, there is a need to better understand the mechanisms through which food, satiation signals, and drugs of abuse engage hypothalamic neurons *in vivo*.

Because alcohol both is a drug and contains calories, we first explored how it affects hypothalamic neural activity and behavior. Our data demonstrate that alcohol robustly inhibits AgRP neuron activity and suggest that alcohol is not detected by the brain as calories—consistent with the lack of effects observed on long-term feeding behavior and body weight regulation following alcohol administration. Furthermore, vagal lesions abolish the effects of post-prandial satiation signals or intragastric lipid infusions on AgRP neuron activity, but the activity reductions by alcohol remain intact. Consistent with alcohol utilizing a calorie-independent "drug" pathway, we discovered that other drugs of abuse inhibit both AgRP and POMC neuron activity, further demonstrating a nutrient-independent mechanism for the inhibition of *in vivo* hypothalamic neuron activity. Finally, we describe a coordinated, bidirectional modulation of hypothalamic hunger and midbrain reward circuits that is substantiated by the ability of AgRP neuron activity to potentiate DA release and the ability of DA signaling to potentiate the inhibition of AgRP neuron activity. Taken together, our results demonstrate that non-nutritive, rewarding substances regulate homeostatic feeding systems and that interdependent modulation of hypothalamic and reward circuits process natural and drug rewards.

## RESULTS

### Intragastric Alcohol Robustly Decreases AgRP Neuron Activity in Awake, Behaving Mice

Recent data demonstrate that calories inhibit AgRP neuron activity (Beutler et al., 2017; Su et al., 2017). Since alcohol has significant calorie content, we reasoned that it may also affect neural activity in hypothalamic feeding circuits. To test this hypothesis, we used fiber photometry to monitor calcium dynamics in hypothalamic neurons following intragastric infusion of alcohol in food-restricted mice (85%–90% free-feeding body weight) (Figure 1A) (Gunaydin et al., 2014; Su et al., 2017). We engineered mice to express the calcium indicator GCaMP6s in AgRP or POMC neurons and measured calcium-dependent fluorescence as a proxy for neural activity and calcium-independent fluorescence as a control for bleaching and movement artifacts (Figures 1A and 1B) (Lerner et al., 2015; Su et al., 2017). Intragastric delivery of ethanol (5% or 15% EtOH in 1 mL) dose-dependently reduced the activity of AgRP neurons (Figures 1C–1E and S1A–S1C), similar to other macronutrients (Beutler et al., 2017; Su et al., 2017). The magnitude of suppression observed with 15% EtOH was 88% of that observed upon chow refeeding (Figure S1D), demonstrating that alcohol is a potent suppressor of AgRP neuron activity.

POMC neuron activity is increased in satiety and responds inversely to AgRP neuron activity (Atasoy et al., 2012; Mandelblat-Cerf et al., 2015). Since food intake activates POMC neuron activity (Figure S2A) (Chen et al., 2015), we hypothesized that intragastric alcohol would increase POMC neuron activity. Surprisingly, intragastric EtOH had no significant effect on POMC neuron activity (Figures 1F–1I and S2B). Consistent with the lack of activation seen in either AgRP or POMC neurons, we found that alcohol did not activate immediate early gene expression in the arcuate nucleus of the hypothalamus (Figure S3). These findings suggest that intragastric alcohol—at least at the level of POMC neurons—signals the brain differently than other nutrients.

### Voluntary Alcohol Drinking Reduces AgRP Neuron Activity but Does Not Entrain Predictive Changes in Neural Activity

Because alcohol is normally self-ingested, we next tested how alcohol drinking affects hypothalamic neuron activity (Figure 2A). We habituated mice for 1 week to a 10% EtOH solution and then monitored AgRP neuron activity during EtOH drinking. AgRP neuron activity was significantly decreased 15 min following EtOH presentation (Figures 2B–2G). The magnitude of this effect reflects the total amount of alcohol consumed, regardless of route of administration. In other words, maximum AgRP neuron activity changes were similar with comparable doses of oral and gastric alcohol (0.04 g ± 0.005 g EtOH drinking versus 0.04 g EtOH IG; Figures 1C and 2B). EtOH drinking did not affect POMC neuron activity (Figures S4A–S4E), consistent with the lack of effects of intragastric EtOH on POMC neuron activity. The lack of effect of alcohol on POMC neuron activity is not due to low alcohol consumption. In fact, these mice consumed significantly more EtOH than the *Agrp*-IRES-Cre mice (Figure S4F), in which there was a significant neural activity change (Figure 2).

Because repeated exposure to nutrients leads to an anticipatory change in AgRP and POMC neuron activity (Betley et al., 2015; Chen et al., 2015; Mandelblat-Cerf et al., 2015), we next examined whether alcohol can condition anticipatory neural responses. We monitored AgRP neuron activity in mice while they were given exposure to either glucose or EtOH solutions. As expected, we found that AgRP neuron activity was reduced on the first exposure to glucose (Figures 2H and 2I). We noted that naive exposure to glucose does not lead to a preemptive change in the neural activity of AgRP neurons that precedes the first lick (Figures 2J–2L). However, subsequent exposures resulted in a preemptive reduction in AgRP neuron activity at the presentation of the glucose spout, before the mice took their first lick (Figures 2K and 2L). In contrast, mice did not exhibit a sensory cue (sight, smell, or taste)-induced suppression of AgRP neuron activity in response to EtOH, despite a week of prior exposure (Figures 2K and 2L). The inability for alcohol to condition AgRP neuron activity responses suggests different pathways for neural integration following ingestion of alcohol and nutrients.

AgRP neuron activity drives consumption of food (Aponte et al., 2011; Krashes et al., 2011). We reasoned that if mice detect alcohol as a caloric substance, activating AgRP neurons should drive alcohol drinking. We thus tested if optogenetic AgRP neuron stimulation supports increased alcohol intake (Figure 2M). AgRP neuron stimulation did not affect EtOH intake but robustly increased glucose intake (Figures 2N and 2O). This is not likely due to the unpleasant taste of alcohol, as mice drank glucose that was devalued with an aversive concentration of quinine (0.3 mM, Figure 2P) (Grobe and Spector, 2008; Mura et al., 2018). If mice calculate the caloric value of alcohol, one prediction would be that they consume less of a glucose/EtOH mixture

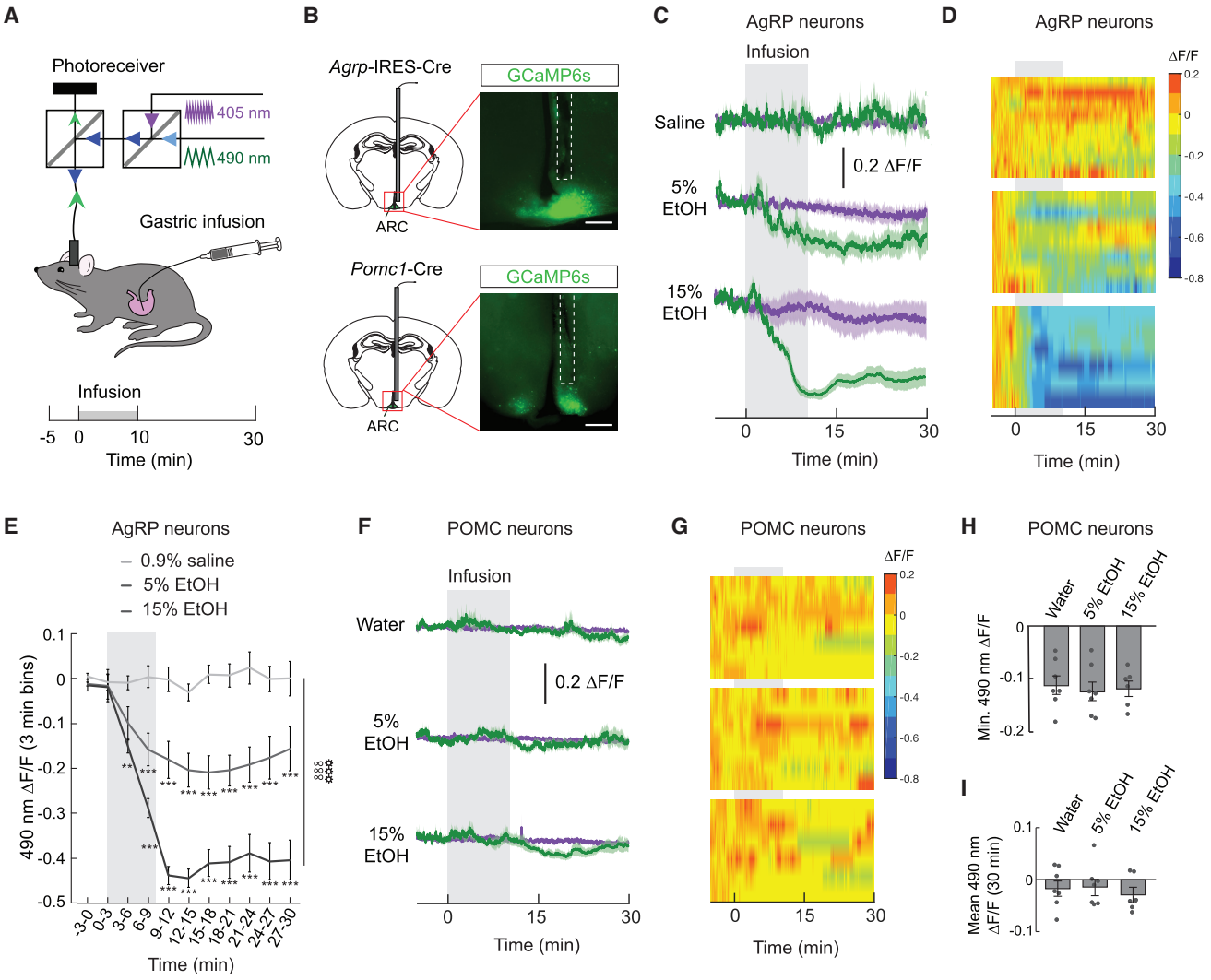


**Figure 1. Intragastric Alcohol Decreases *In Vivo* AgRP Neuron Activity**

(A) Dual-wavelength fiber photometry (FP) setup used to record calcium-dependent fluorescence (excited at 490 nm) and calcium-independent fluorescence (excited at 405 nm) in mice during intragastric infusion of ethanol (EtOH).

(B) Schematics for monitoring calcium dynamics in hypothalamic neurons, and representative image of GCaMP6s in AgRP (top) and POMC (bottom) neurons. Scale bars, 500 μm.

(C) Average ΔF/F of GCaMP6s signals in AgRP neurons of food-restricted mice infused with saline (n = 9), 5% EtOH (n = 7), or 15% EtOH (n = 6). Signals are aligned to the start of infusion. Green, 490 nm signal; purple, 405 nm control signal. Darker lines represent means, and lighter shaded areas represent SEMs.

(D) Heatmaps reporting ΔF/F of the 490 nm signal of the recordings in individual mice in (C).

(E) Mean ΔF/F of the 490 nm signal in 3 min bins from mice infused with EtOH in (C) (n = 6–9/group, two-way repeated-measures ANOVA, $p < 0.001$).

(F) Average ΔF/F of GCaMP6s signals in POMC neurons of food-restricted mice infused with water (n = 7), 5% EtOH (n = 7), or 15% EtOH (n = 6).

(G) Heatmaps reporting ΔF/F of the 490 nm signal of individual mice in (F) (n = 7/group).

(H) Minimum ΔF/F of the 490 nm signal following gastric infusion of mice in (F) (n = 6–7/group, one-way ANOVA, p = ns).

(I) Mean ΔF/F of the 490 nm signal from 0 to 30 min following gastric infusion of mice in (F) (n = 6–7/group, one-way ANOVA, p = ns). Data are expressed as mean ± SEM, ns $p > 0.05$, t tests and post hoc comparisons: $^{**}p < 0.01$, $^{***}p < 0.001$; ANOVA interaction: ∞ ∞ ∞ $p < 0.001$; ANOVA main effect of group: ☼☼☼ $p < 0.001$. See also Figures S1–S3.

(0.32 kcal/mL, 0.16 kcal/mL from glucose, and 0.16 kcal/mL from EtOH) compared to just glucose (0.16 kcal/mL). Interestingly, AgRP neuron stimulation drives similar consumption of both solutions, despite the major calorie difference (Figure 2Q). Taken together, these data suggest that the brain does not associate alcohol with calories at the level of AgRP neurons.

## Alcohol Reduces AgRP Neuron Activity through a Vagal-Independent Pathway

To explore the mechanistic differences that mediate the effects of alcohol and nutrients on AgRP neuron activity, we examined the role of vagal gut-brain signaling. Nutrients act in the gastrointestinal (GI) tract to release satiation signals such as CCK

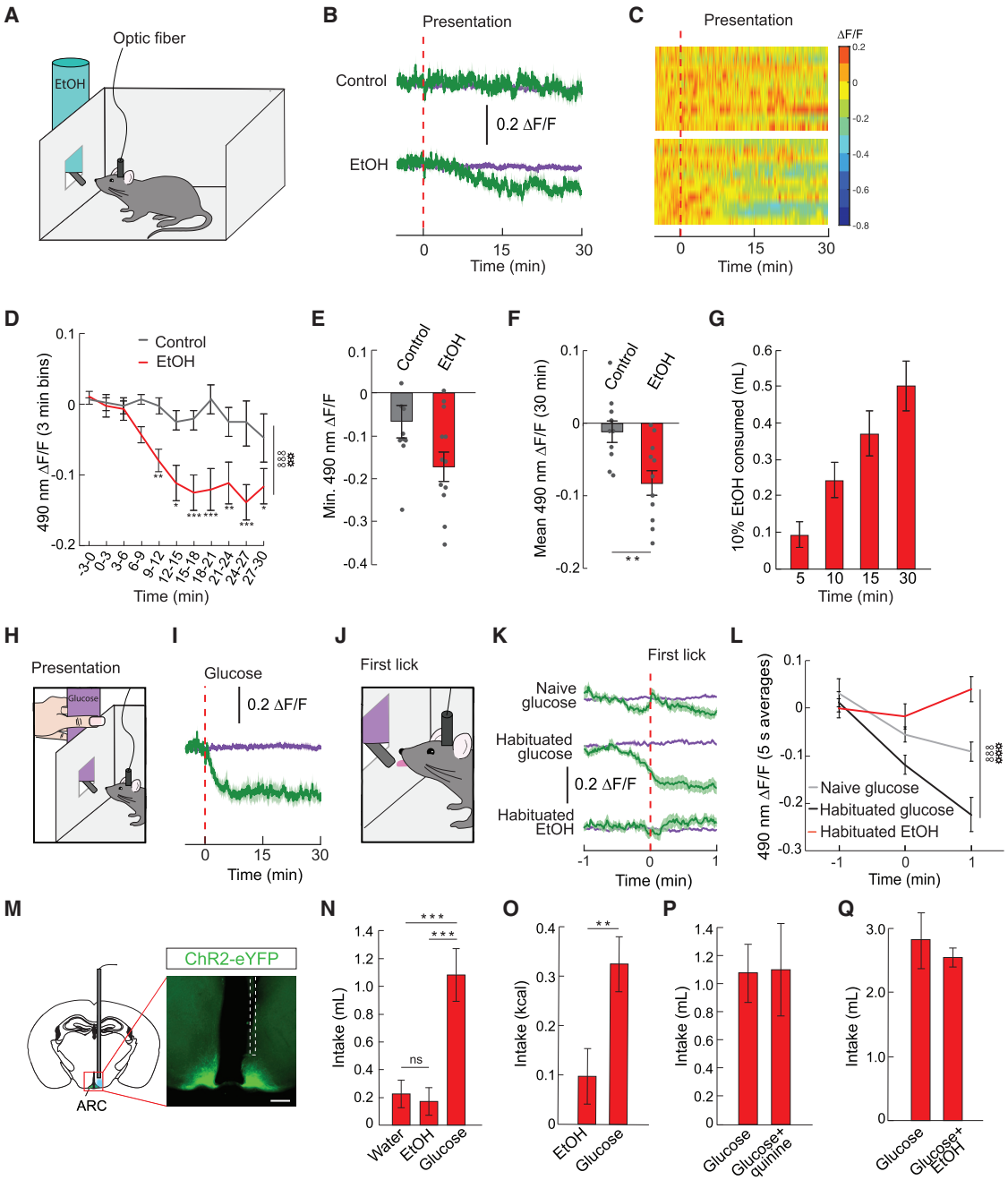


**Figure 2. Alcohol, Unlike Glucose, Does Not Condition a Preemptive Change in AgRP Neuron Activity**

(A) Habituated, food-restricted mice were given 10% EtOH or control solution, and AgRP or POMC neuron activity was recorded.

(B) Average ΔF/F of GCaMP6s signals in AgRP neurons of food-restricted mice drinking 10% EtOH (n = 11) or control (n = 10) solutions. Signals are aligned to the presentation of solution. Green, 490 nm signal; purple, 405 nm control signal. Darker lines represent means, and lighter shaded areas represent SEMs.

(C) Heatmaps reporting ΔF/F of the 490 nm signal of the recordings in individual mice in (B).

(D) Mean ΔF/F of the 490 nm signal in 3 min bins from mice drinking 10% EtOH (n = 10–11/group, two-way repeated-measures ANOVA, $p < 0.001$).

(E) Minimum ΔF/F of the 490 nm signal following EtOH drinking (n = 10–11/group, one-way ANOVA, p = ns).

(F) Mean ΔF/F of the 490 nm signal from 0 to 30 min following EtOH drinking (n = 10–11/group, one-way ANOVA, $p < 0.01$).

(G) Cumulative 10% EtOH consumed over recording period.

(H) Naive, food-restricted mice were presented with glucose (14%, equicaloric to 10% EtOH), and AgRP or POMC neuron activity was recorded. Data were aligned to the presentation of glucose.

(I) Average ΔF/F of GCaMP6s signals in AgRP neurons of food-restricted mice following presentation of glucose (n = 13).

*(legend continued on next page)*

(cholecystokinin) and peptide YY (PYY). It has recently been shown that these signals rapidly and robustly reduce AgRP neuron activity (Beutler et al., 2017; Su et al., 2017). CCK and PYY are thought to act at least in part through action on the vagus nerve, which in turn rapidly transmits GI signals to the brain (Bhavsar et al., 1998; Kopin et al., 1999; Neary et al., 2005). Additionally, PYY has been shown to act directly on AgRP neurons (Batterham et al., 2002). To determine whether vagal neurotransmission mediates fast communication between the gut and AgRP neurons, we first tested the effects of satiation signals on *in vivo* AgRP neuron activity in mice following a complete subdiaphragmatic vagotomy (VGX). In this preparation, we resected and cauterized all afferent and efferent subdiaphragmatic vagal fibers, eliminating the contribution of vagal neurotransmission (Figure 3A). As previously shown, VGX significantly attenuated the intake-suppressive effects of CCK (Figure 3B) and abolished Fluoro-Gold transport from the gut to the dorsal motor nucleus of the vagus (DMX) (Figure 3C), verifying our vagal lesion (Flood et al., 1987; Joyner et al., 1993; Powley et al., 1987). VGX eliminated the effects of CCK and PYY on AgRP neuron activity (Figures 3D–3G, S5A, and S5B), suggesting that vagal neurotransmission, but not direct central action of these signals, mediates the suppression of AgRP neuron activity. Furthermore, the ability of intragastric fat to reduce AgRP neuron activity was dramatically attenuated following VGX (Figures 3H–3J, Figure S5C). In striking contrast, the effect of intragastric EtOH on AgRP neuron activity was intact following vagotomy (Figures 3H, 3I, 3K, and S5D), demonstrating that fat or satiation signals and alcohol inhibit AgRP neuron activity via distinct gut-brain pathways.

Since the effects of alcohol are not vagally mediated and alcohol crosses the blood brain barrier, we next tested the ability of alcohol to modulate AgRP neuron activity when infused directly into the brain (Figure S6A). While recording the calcium dynamics of AgRP neurons, we infused EtOH (0.8 μg) into the lateral ventricle and found that AgRP neuron activity rapidly and robustly decreased (Figures S6B–S6D). Taken together, these findings suggest that the drug action of alcohol on AgRP neuron activity can occur through direct action in the brain.

## Alcohol Acutely Reduces Food Intake in Food-Deprived, but Not *Ad Libitum*-Fed, Mice

Previous studies have reported contradictory effects of alcohol on food intake. To explore short-term (hours) and chronic (2 weeks) effects of alcohol, we performed intragastric infusions or i.p. injections of EtOH and measured food intake. In *ad libitum*-fed mice, neither intragastric (5% or 15%, Figure 4A) nor i.p. (2 g/kg, Figure 4B) EtOH significantly affected food intake up to 24 h post-administration, although we observed short-term trends for intake reductions following IG EtOH. In contrast, food-deprived mice show a marked suppression of food intake following EtOH administration (Figures 4C and 4D). To explore the possibility that long-term exposure to alcohol affects energy balance, we administered i.p. EtOH daily (2 g/kg per day) for 2 weeks while measuring food intake and body weight. Similar to acute exposure to EtOH, 2 weeks of EtOH injections did not affect food intake or body weight (Figures 4E and 4F). These data show that alcohol reduces food intake in food-deprived mice, consistent with the observed alcohol-induced reductions in AgRP neuron activity in hungry mice.

## Alcohol Concurrently Affects Homeostatic and Reward Signaling

Since alcohol intake is known to increase dopamine signaling (Gessa et al., 1985), we measured calcium dynamics in ventral tegmental area (VTA) dopamine (DA) neurons (Figure 5A) during peripheral administration of alcohol. As expected, we found intragastric infusion of EtOH increased DA neuron activity (Figures 5B–5F). In light of our contradictory findings on the inhibitory effect of alcohol on AgRP neuron activity relative to previous reports (Cains et al., 2017), these results rule out the possibility that alcohol universally inhibits calcium signaling in the brain. This increase in DA neuron activity occurs without any sensory association or training, as EtOH increased DA neuron activity on the first trial (Figures 5B–5F). Similarly, intragastric fat also increased DA neuron activity on the first trial (Figures 5B–5F), suggesting that detection of either of these substances intrinsically activates reward pathways in the brain. This demonstrates that alcohol and nutrients communicate with both homeostatic and reward systems in the absence of external or interoceptive sensory cues. Although we observed increases in DA neuron activity with both intragastric nutrients and alcohol, the time course of DA neuron activation was different despite their similar calorie content (time to average maximum ΔF/F from start of infusion: EtOH, 600 s; fat, 264 s) (Figures 5B and 5D). Importantly, differences between alcohol and fat were also observed in striatal DA signaling (DA sensor; Sun et al., 2018), as EtOH, but not fat, significantly increased nucleus accumbens (NAc) dopamine signaling (Figures 5G–5L). Conversely, fat, but not EtOH, significantly increased dorsal striatum DA signaling (Figures 5M–5R) (Han et al., 2018). The inability of fat to increase NAc DA signaling suggests that VTA neurons that project outside of the NAc are activated by fat, while VTA neurons activated by EtOH project

(J) Food-restricted mice were presented with 14% glucose (naive), 14% glucose (habituated), or 10% EtOH (habituated), and AgRP neuron activity was recorded. Data are aligned to the first lick.

(K) Average ΔF/F of GCaMP6s signals in AgRP neurons of food-restricted mice following first lick of glucose or EtOH (n = 8–13/group).

(L) Average ΔF/F (5 s average) of the 490 nm signal before the first lick. Data are aligned to first lick at time = 0 min (n = 8–13/group, two-way repeated-measures ANOVA, $p < 0.001$).

(M) Schematic for optogenetic activation of AgRP neurons, and representative image of ChR2 in AgRP neurons. Scale bar, 500 μm.

(N) Water, EtOH, and glucose intake (in mL) during 1 h of AgRP neuron stimulation (n = 11/group, one-way repeated-measures ANOVA, $p < 0.001$).

(O) EtOH and glucose intake (in kcal) during 1 h of AgRP neuron stimulation (n = 11/group, paired t test, $p < 0.01$).

(P) Glucose intake with and without 0.3 mM quinine during 1 h of AgRP neuron stimulation (n = 6/group, paired t test, p = ns).

(Q) Glucose (0.16 kcal/mL) or glucose + EtOH intake (0.32 kcal/mL, 0.16 kcal/mL glucose, and 0.16 kcal/mL EtOH) during 1 h of AgRP neuron stimulation (n = 6/group, paired t test, p = ns). Data are expressed as mean ± SEM, ns $p > 0.05$, t tests and post hoc comparisons: **$p < 0.01$, ***$p < 0.001$; ANOVA interaction: ∞ ∞ ∞ $p < 0.001$; ANOVA main effect of group: ☼☼☼ $p < 0.001$. See also Figure S4.

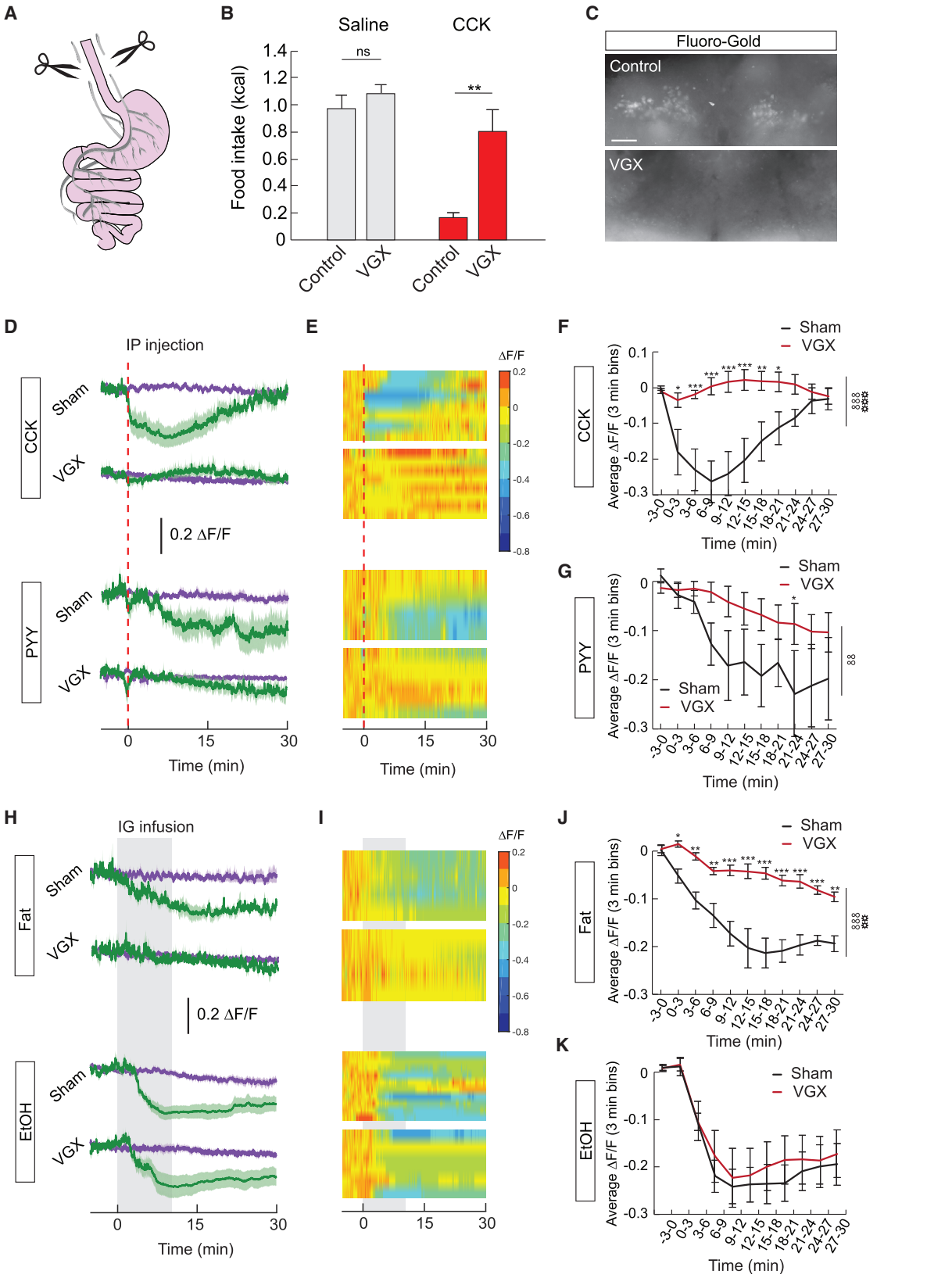


*(legend on next page)*

to the NAc. Together with the effects of alcohol observed in AgRP and POMC neurons, these data suggest that alcohol and nutrients differentially modulate these circuits.

### Drugs of Abuse Concomitantly Reduce *In Vivo* AgRP and POMC Neuron Activity Dynamics and Increase Mesoaccumbal Dopamine Signaling

Given that the effects of alcohol on hypothalamic neuron activity do not seem to be driven by caloric content, we reasoned that other drugs of abuse may have similar effects. We thus examined the ability of several drugs with appetite-suppressive effects (Epstein, 1959) to affect AgRP and POMC neuron activity. We found that i.p. injection of cocaine, amphetamine, and nicotine decrease AgRP and POMC neuron activity levels (Figures 6A–6H), and these responses were consistent among individuals (Figures 6B and 6F). Importantly, these drugs of abuse do not contain significant amounts of calories, further demonstrating a nutrient-independent mechanism that mediates sustained changes in *in vivo* hypothalamic neuron activity. In contrast, i.p. injection of glucose did not significantly affect AgRP or POMC neuron activity (Figures 6A–6H). Taken together, these findings suggest that caloric substances require passage through the GI tract to influence hypothalamic neuron activity, while drugs of abuse use a distinct mechanism that likely involves direct action in the brain.

Drugs of abuse that modulate AgRP/POMC neuron activity (Figures 6A–6H) are also known to stimulate dopamine signaling. We thus tested the same doses of these drugs for their ability to increase VTA DA neuron activity and NAc DA signaling. Consistent with effects on AgRP and POMC neurons, saline, glucose, and caffeine had no significant effect on VTA dopamine neuron activity (GCaMP6f; Figures 6I–6L) or NAc DA signaling (Figures 6M–6P). Cocaine, amphetamine, and nicotine each increased DA signaling in the NAc (Figures 6M–6P). As previously shown, nicotine increased but cocaine decreased DA neuron activity (Figures 6I–6L), due to cocaine-induced feedback inhibition onto these neurons (Brodie and Dunwiddie, 1990; Mejías-Aponte and Kiyatkin, 2012). Together, these data demonstrate the concurrent regulation of hypothalamic and reward circuits by drugs of abuse, suggesting an interaction between these systems in the processing of natural and drug rewards.

### Interdependent Modulatory Effects of AgRP and DA Signaling

Because hunger potentiates the rewarding value of natural and drug rewards (Cabeza de Vaca and Carr, 1998; Carr, 2002; Cone et al., 2014), we next examined the role of AgRP neuron activity on NAc DA signaling in *ad libitum*-fed mice. We stimulated AgRP neurons using excitatory designer receptors exclusive activated by designer drugs (DREADDs, hM3Dq) while measuring the DA response to food and drugs (Figures 7A and 7B). As previously shown (Krashes et al., 2011), activation of AgRP neurons via i.p. injection of clozapine N-oxide (CNO) significantly increased food intake (Figure 7C). AgRP neuron activation potentiated the DA response to food (Figures 7D–7F), an effect not observed in mice lacking DREADDs in AgRP neurons (Figure S7A). DA responses to drugs were also potentiated following AgRP neuron stimulation (Figures 7G–7L and S7B–S7E). The potentiation of DA signaling by AgRP neuron activity is dependent on the receipt of rewards, as AgRP neuron stimulation without reward does not alter DA levels (Figures S8A–S8E).

To determine if the interaction between AgRP and DA signaling is bidirectional, we next modulated DA signaling while monitoring AgRP neuron activity dynamics in food-restricted mice (Figures 8A and 8B). Reducing DA signaling with an i.p. injection of D1 and D2 receptor antagonists attenuated AgRP neuron inhibition in response to IG infusion of fat (Figures 8C–8E, S7F, and S7G). Additionally, DA receptor antagonism diminished AgRP neuron responses to alcohol and nicotine (Figures 8F–8K and S7H–S7K). Again, these changes are dependent upon reward delivery, as DA antagonists had no direct effect on AgRP neuron activity (Figures S8F–S8J). Taken together, these data demonstrate bidirectional, modulatory effects of AgRP and DA signaling in response to both natural and drug rewards.

## DISCUSSION

Here, we show vagal-dependent and -independent modes for signaling rewards to the brain and reveal bidirectional, modulatory network effects across hypothalamic and midbrain circuits. We demonstrate that AgRP and POMC neuron activity

**Figure 3. Alcohol Does Not Require Vagal Gut-Brain Signaling to Reduce AgRP Neuron Activity**

(A) A complete subdiaphragmatic vagotomy (VGX) was performed prior to *in* vivo neural activity recordings in mice.

(B) Food intake in control and VGX mice following i.p. injection of CCK (n = 4/group, two-way repeated-measures ANOVA, main effect of group $p < 0.01$).

(C) Representative image of Fluoro-Gold in the DMX of control (top) and VGX (bottom) mice. Scale bar, 100 μm.

(D) Average ΔF/F of GCaMP6s signals in AgRP neurons of sham or VGX mice following i.p. injection of CCK or PYY (n = 7/group). Signals are aligned to i.p. injection. Green, 490 nm signal; purple, 405 nm control signal. Darker lines represent means, and lighter shaded areas represent SEMs.

(E) Heatmaps reporting ΔF/F of the 490 nm signal of the recordings in individual mice in (D).

(F) Mean ΔF/F of the 490 nm signal (3 min bins) in AgRP neurons in sham or VGX mice following i.p. injection of CCK (n = 7/group, two-way repeated-measures ANOVA, $p < 0.001$).

(G) Mean ΔF/F of the 490 nm signal (3 min bins) in AgRP neurons in sham or VGX mice following i.p. injection of PYY (n = 4–6/group, two-way repeated-measures ANOVA, $p < 0.01$).

(H) Average ΔF/F of GCaMP6s signals in AgRP neurons of sham or VGX mice following intragastric infusion of fat or EtOH (n = 4/group).

(I) Heatmaps reporting ΔF/F of the 490 nm signal of the recordings in individual mice in (H).

(J) Mean ΔF/F of the 490 nm signal (3 min bins) in AgRP neurons in sham or VGX mice following intragastric infusion of fat (n = 4/group, two-way repeated-measures ANOVA, $p < 0.001$).

(K) Mean ΔF/F of the 490 nm signal (3 min bins) in AgRP neurons in sham or VGX mice following intragastric infusion of EtOH (n = 6–10/group, two-way repeated-measures ANOVA, p = ns). Data are expressed as mean ± SEM, ns $p > 0.05$, t tests and post hoc comparisons: *$p < 0.05$, **$p < 0.01$, ***$p < 0.001$; ANOVA interaction: ∞∞$p < 0.01$, ∞∞∞$p < 0.001$; ANOVA main effect of group: ☼☼$p < 0.01$, ☼☼☼$p < 0.001$. See also Figures S5 and S6.

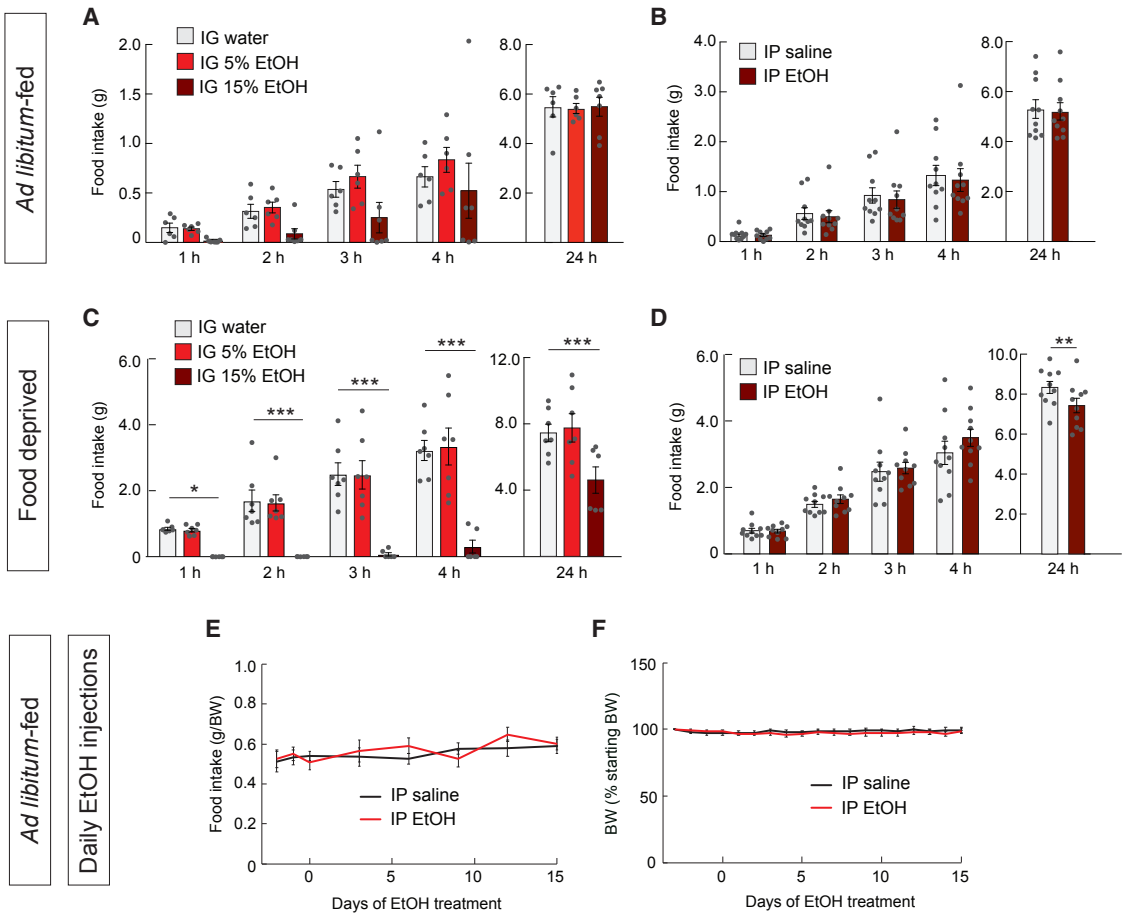


**Figure 4. Alcohol Acutely Reduces Food Intake in Food-Deprived, but Not *Ad Libitum*-Fed, Mice**

(A) Food (chow) intake following intragastric infusion of EtOH in *ad libitum*-fed mice (n = 6–7/group, two-way repeated-measures ANOVA, p = ns).

(B) Food intake following i.p. injection of EtOH in *ad libitum*-fed mice (n = 10/group, two-way repeated-measures ANOVA, p = ns).

(C) Food intake following intragastric infusion of EtOH in 24 h food-deprived mice (n = 6–7/group, two-way repeated-measures ANOVA, $p < 0.01$).

(D) Food intake following i.p. injection of EtOH in 24 h food-deprived (n = 10/group, two-way repeated-measures ANOVA, $p < 0.01$).

(E) Food intake in *ad libitum*-fed mice treated daily with i.p. injection of EtOH (n = 9/group, two-way repeated-measures ANOVA, p = ns).

(F) Body weight (% of original weight) in mice treated daily with i.p. injection of EtOH (n = 9/group, two-way repeated-measures ANOVA, p = ns). Data are expressed as mean ± SEM, ns $p > 0.05$.

is modulated by both natural and drug rewards. By dissociating the signaling modes through which alcohol affects hypothalamic neural activity, we provide evidence that the caloric content of alcohol is not relayed to the brain like other macronutrients. We demonstrate that satiation signals and intragastric fat modulate AgRP neurons in the brain through vagal neurotransmission. Conversely, drugs modulate feeding circuits through a different pathway, likely through direct action on the brain. Further, we demonstrate that hypothalamic AgRP neurons and midbrain dopamine circuits form reciprocal networks that modulate the neural processing of rewards. These findings demonstrate that drugs of abuse not only hijack midbrain reward pathways in the brain but also influence the activity of canonical feeding regulators, such as hypothalamic AgRP and POMC neurons. Taken together, this work provides new insight on the complex and interdependent circuitry that mediates motivated behavior.

## Coordinated Activity in Hypothalamic and Dopamine Circuits in Response to Food and Drug Rewards

We show that a diverse array of drugs of abuse can modulate activity in hypothalamic neurons. Each of the drugs tested (except alcohol) lacks calories yet at least partially recapitulates the effects of nutrients at AgRP neurons. Our data suggest that exogenous substances (i.e., drugs of abuse) can robustly inhibit AgRP neuron activity independent of calories, raising the possibility that pharmacotherapeutics could be used to modulate AgRP neuron activity. In contrast to nutrients, drugs reduce or do not affect POMC neuron activity. These findings were surprising, given that AgRP and POMC neurons typically respond in opposing directions (Atasoy et al., 2012; Mandelblat-Cerf et al., 2015). Similar activity changes at AgRP and POMC neurons, although uncommon, have been previously observed (Huang et al., 2011). One potential explanation for these effects may be the expression of common receptors on

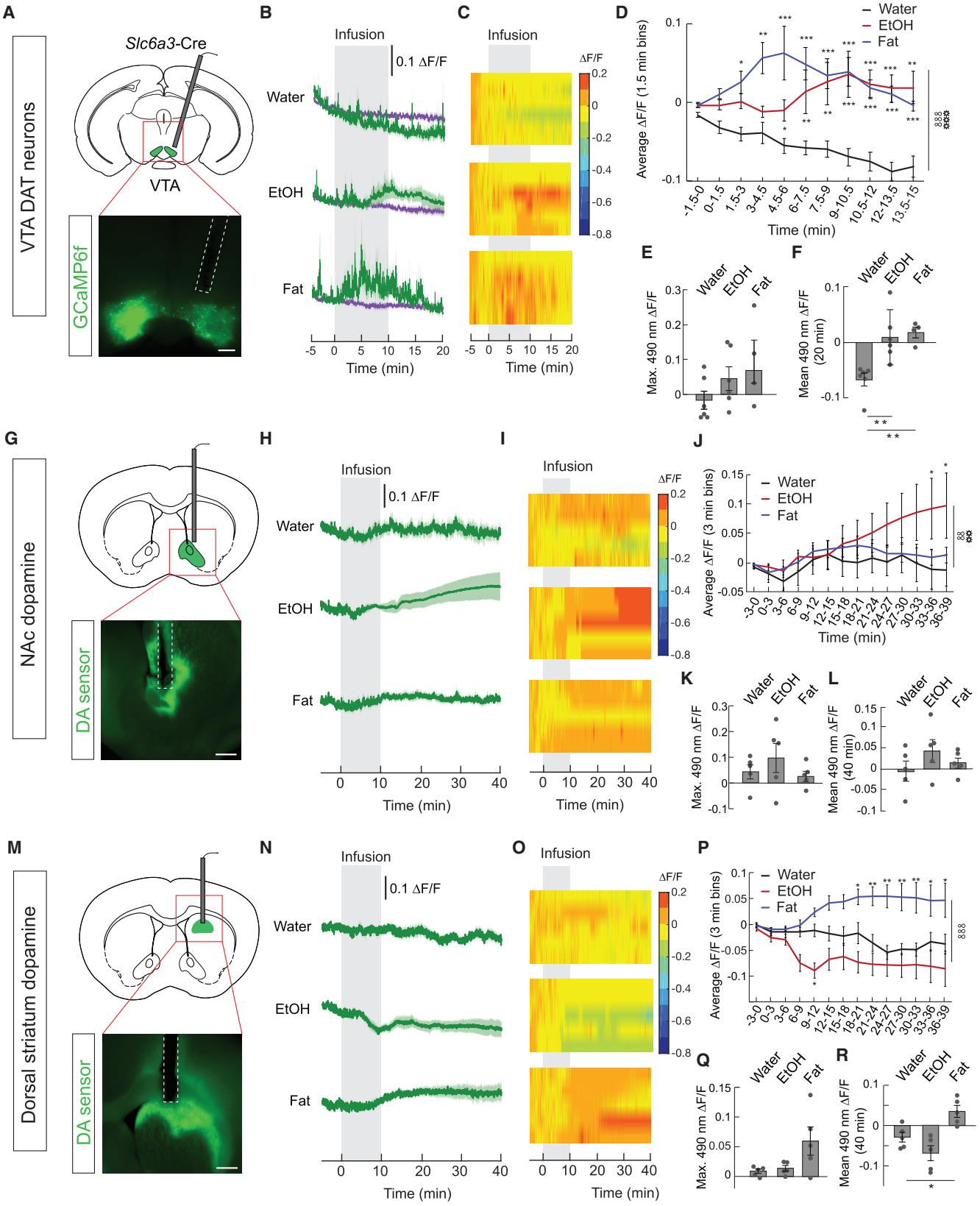


*(legend on next page)*

both AgRP and POMC neurons that are potently activated by drugs of abuse, as is the case for nicotine (Calarco et al., 2018; Calarco and Picciotto, 2019). This dysregulation of hypothalamic neuron activity further supports the notion that nutrients and drugs utilize distinct pathways and may in part contribute to the detrimental effects of drugs on the brain and behavior. For example, the ability of drugs to "hijack" hypothalamic circuitry may shift motivational drives away from natural rewards and toward drug rewards, promoting drug reinforcement. In the future, it will be important to determine if and how drugs of abuse affect neural activity in other brain regions that control food intake, as well as in brain regions that control other homeostatic needs and behavioral drives.

Understanding how reward systems interact with circuits that communicate homeostatic needs remains a major challenge (Rossi and Stuber, 2018). Reward signals are potentiated by hunger (Carr, 2002), and our work here demonstrates that AgRP neuron activity underlies this effect by increasing reward-evoked dopamine signaling. Additionally, food seeking in response to the neural and hormonal changes induced by food deprivation requires a functional reinforcement system (Szczypka et al., 1999; Zhou and Palmiter, 1995), as food reward is devalued in the absence of dopamine signaling (Wise et al., 1978). Our findings provide evidence for the concurrent and interdependent regulation of homeostatic and reward circuits and suggest that concerted neural activity in these circuits influences behavior. Emerging work suggests that the lateral hypothalamus may be an important site of convergence in interfacing between the homeostatic and reward networks of the brain (Stuber and Wise, 2016). Indeed, the lateral hypothalamus forms reciprocal projections with both the arcuate nucleus of the hypothalamus (Betley et al., 2013; Bouret et al., 2004; Broberger et al., 1998; Luan et al., 2017) and the VTA (Geisler et al., 2007; Nieh et al., 2015; Yu et al., 2019). Dissecting the interconnected anatomy and function of the networks formed by these circuits will enable a deeper understanding of how the body signals the brain to meet metabolic demands and ensure survival (Rossi and Stuber, 2018; Saper et al., 2002).

The dramatic reduction in AgRP neuron activity by alcohol and drugs of abuse suggests that the reinforcing effects of drugs may be mediated not only by reward pathways but also by homeostatic loci in the brain. Our findings uncover a potential dual mechanism of reinforcement that enhances drug use—as increased dopamine signaling and decreased AgRP neuron activity both increase affect (Betley et al., 2015; Volkow et al., 2017). Coordinated changes to these two systems may serve to increase the positive affect associated with food intake and drug use—with clinical implications for diseases such as obesity and drug addiction.

## Alcohol and Food Intake

Alcohol contributes to energy intake without providing any essential nutrients (Schutz, 2000). Although alcohol contains calories (7 kcal/g), the mechanisms responsible for the metabolism of alcohol are different than those mediating the metabolism of other macronutrients (Cederbaum, 2012). While the role of alcohol as a food has been examined, whether and how alcohol affects food intake has remained contentious (Cains et al., 2017; Gill et al., 1996; Hetherington et al., 2001; Richter, 1941, 1953). Here, we observed an acute reduction in food intake following high doses of alcohol in mice that were food deprived. However, there were no significant changes in food intake in *ad libitum*-fed mice, even after 2 weeks of daily alcohol exposure. This lack of change in food intake and body weight occurs despite extra calories from alcohol. However, the caloric contribution of alcohol in our studies is relatively minor (1/3–1 kcal/day; or approximately 2%–6% of total daily caloric intake) and thus may not have an additive effect that manifests in body weight changes, at least for up to 2 weeks of alcohol administration. Additionally, energy expenditure is increased following administration of alcohol

**Figure 5. Nutrients and Alcohol Increase Dopamine Signaling**

(A) Schematic for monitoring calcium dynamics in dopamine neurons, and representative image of GCaMP6f in neurons expressing dopamine active transporter (*Slc6a3*, DAT neurons). Scale bar, 500 μm.

(B) Average ΔF/F of GCaMP6f signals in DAT neurons of food-restricted mice following intragastric infusion of water (n = 6), EtOH (n = 6), or fat (n = 4).

(C) Heatmaps reporting ΔF/F of the 490 nm signal of individual mice in (B).

(D) Mean ΔF/F of the 490 nm signal in 90 s bins from mice infused with EtOH, fat, or water in (B) (n = 4–6/group, two-way repeated-measures ANOVA, $p < 0.001$).

(E) Maximum ΔF/F of the 490 nm signal following gastric infusion of mice in (B) (n = 4–6/group, one-way ANOVA, p = ns).

(F) Mean ΔF/F of the 490 nm signal from 0 to 20 min following gastric infusion of mice in (B) (n = 4–6/group, one-way ANOVA, $p < 0.01$).

(G) Schematic for monitoring dopamine signaling in the nucleus accumbens (NAc), and representative image of neurons expressing the dopamine (DA) sensor. Scale bar, 500 μm.

(H) Average ΔF/F of DA sensor in food-restricted mice following intragastric infusion of water, EtOH, or fat (n = 5/group).

(I) Heatmaps reporting ΔF/F of the 490 nm signal of the recordings in individual mice in (H).

(J) Mean ΔF/F of the 490 nm signal in 3 min bins from mice infused with EtOH, fat, or water in (H) (n = 5/group, two-way repeated-measures ANOVA, $p < 0.01$).

(K) Maximum ΔF/F of the 490 nm signal following gastric infusion of mice in (H) (n = 5/group, one-way ANOVA, p = ns).

(L) Mean ΔF/F of the 490 nm signal from 0 to 40 min following gastric infusion of mice in (H) (n = 5/group, one-way ANOVA, p = ns).

(M) Schematic for monitoring dopamine signaling in the dorsal striatum, and representative image of neurons expressing the dopamine (DA) sensor. Scale bar, 500 μm.

(N) Average ΔF/F of DA sensor in food-restricted mice following intragastric infusion of water, EtOH, or fat (n = 5/group).

(O) Heatmaps reporting ΔF/F of the 490 nm signal of the recordings in individual mice in (N).

(P) Mean ΔF/F of the 490 nm signal in 3 min bins from mice infused with EtOH, fat, or water in (N) (n = 5/group, two-way repeated-measures ANOVA, $p < 0.001$).

(Q) Maximum ΔF/F of the 490 nm signal following gastric infusion of mice in (N) (n = 5/group, one-way ANOVA, p = ns).

(R) Mean ΔF/F of the 490 nm signal from 0 to 40 min following gastric infusion of mice in (N) (n = 5/group, one-way ANOVA, $p < 0.05$). Data are expressed as mean ± SEM, ns $p > 0.05$, t tests and post hoc comparisons: *$p < 0.05$, **$p < 0.01$, ***$p < 0.001$; ANOVA interaction: ∞∞$p < 0.01$, ∞∞∞$p < 0.001$; ANOVA main effect of group: ☼☼$p < 0.01$, ☼☼☼$p < 0.001$.

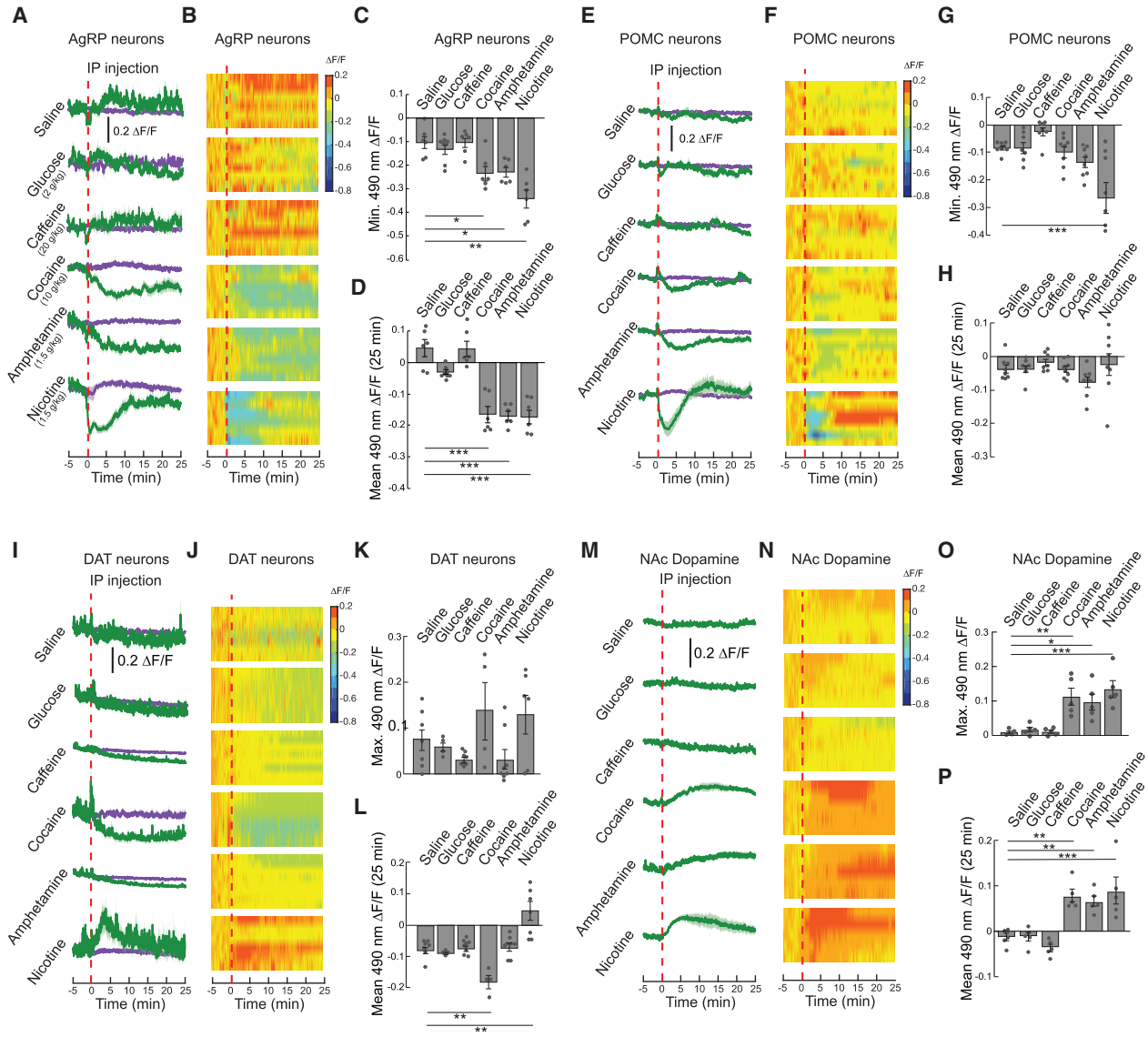


**Figure 6. Drugs of Abuse Inhibit AgRP and POMC Neuron Activity and Potentiate Dopamine Signaling**

(A) Average ΔF/F of GCaMP6s signals in AgRP neurons following i.p. injection of saline, glucose (2 g/kg), caffeine (20 mg/kg), cocaine (10 mg/kg), amphetamine (1.5 mg/kg), or nicotine (1.5 mg/kg) (n = 6–8/group). Signals are aligned to i.p. injection. Green, 490 nm signal; purple, 405 nm control signal. Darker lines represent means, and lighter shaded areas represent SEMs.

(B) Heatmaps reporting ΔF/F of the 490 nm signal of the recordings in individual mice in (A).

(C) Minimum ΔF/F of the 490 nm signal following i.p. injection of mice in (A) (n = 6–8/group, one-way ANOVA, $p < 0.001$).

(D) Mean ΔF/F of the 490 nm signal from 0 to 25 min following i.p. injection of mice in (A) (n = 6–8/group, one-way ANOVA, $p < 0.001$).

(E) Average ΔF/F of GCaMP6s signals in POMC neurons following i.p. injection of glucose or drugs (n = 7–8/group).

(F) Heatmaps reporting ΔF/F of the 490 nm signal of the recordings in individual mice in (E).

(G) Minimum ΔF/F of the 490 nm signal following i.p. injection of mice in (E) (n = 7–8/group, one-way ANOVA, $p < 0.001$).

(H) Mean ΔF/F of the 490 nm signal from 0 to 25 min following i.p. injection of mice in (E) (n = 7–8/group, one-way ANOVA, p = ns).

(I) Average ΔF/F of GCaMP6f signal in neurons expressing dopamine active transporter (DAT neurons) following i.p. injection of glucose or drugs (n = 4–8/group).

(J) Heatmaps reporting ΔF/F of the 490 nm signal of the recordings in individual mice in (I).

(K) Maximum ΔF/F of the 490 nm signal following i.p. injection of mice in (I) (n = 4–8/group, one-way ANOVA, $p < 0.05$).

(L) Mean ΔF/F of the 490 nm signal from 0 to 25 min following i.p. injection of mice in (I) (n = 4–8/group, one-way ANOVA, $p < 0.001$).

(M) Average ΔF/F of neurons expressing a dopamine (DA) sensor in the nucleus accumbens (NAc) following i.p. injection of glucose or drugs (n = 5/group).

(N) Heatmaps reporting ΔF/F of the 490 nm signal of the recordings in individual mice in (M).

(O) Maximum ΔF/F of the 490 nm signal following i.p. injection of mice in (M) (n = 5/group, one-way ANOVA, $p < 0.001$).

(P) Mean ΔF/F of the 490 nm signal from 0 to 25 min following i.p. injection of mice in (M) (n = 5/group, one-way ANOVA, $p < 0.001$). Data are expressed as mean ± SEM, ns $p > 0.05$, t tests and post hoc comparisons: *$p < 0.05$, **$p < 0.01$, ***$p < 0.001$.

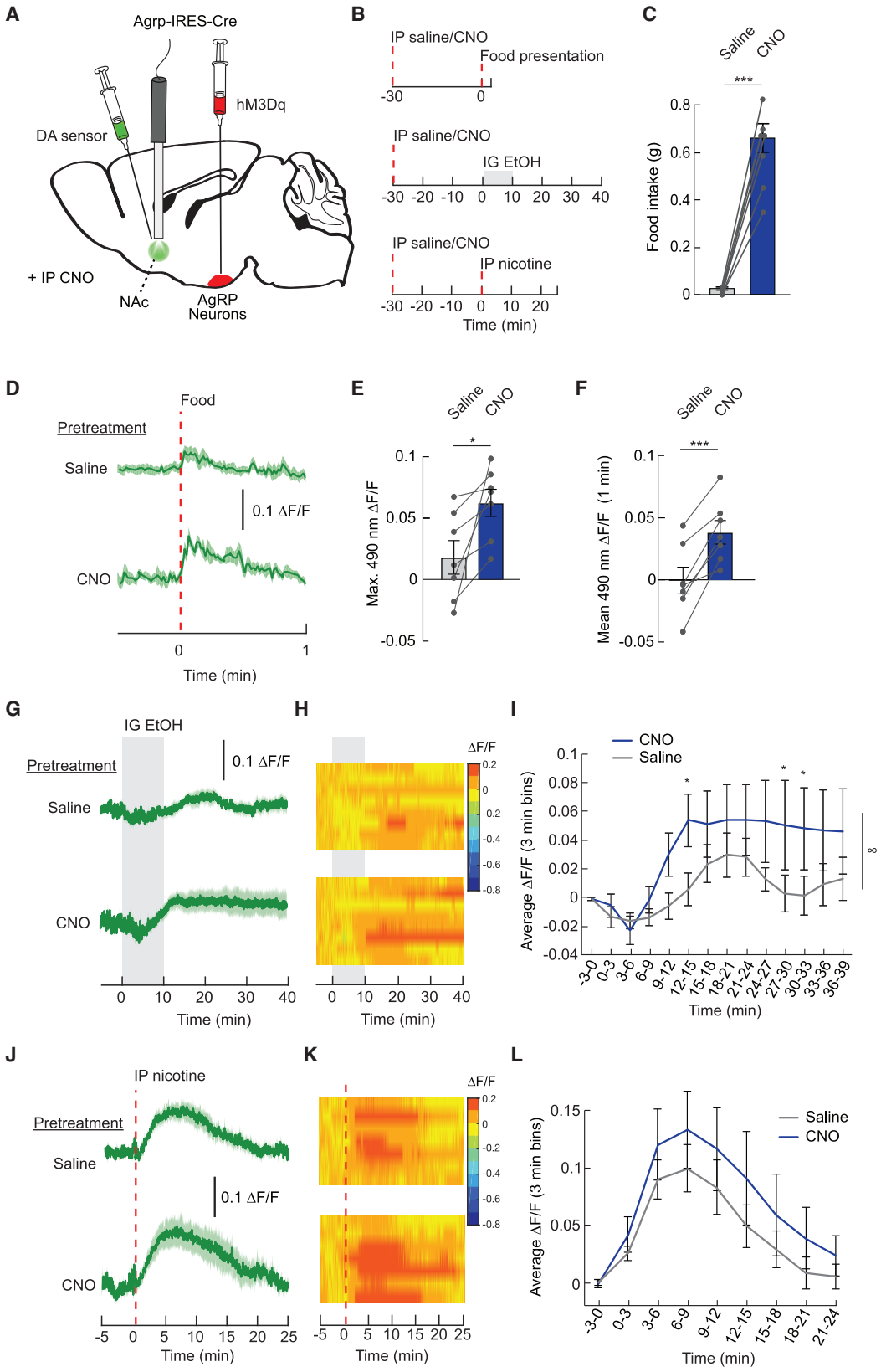


(legend on next page)

(Raben et al., 2003; Rothwell and Stock, 1984; Suter et al., 1994), which has a larger thermogenic effect compared to macronutrients and is less efficient as an energy source (Schutz, 2000; Weststrate et al., 1990). This increase in thermogenesis may help explain why we do not observe weight gain in mice who are given chronic alcohol. Overall, the results of our food intake measurements, along with those from previous reports (Poppitt et al., 1996; Tremblay et al., 1995), suggest that the caloric value of alcohol is not computed by AgRP and POMC neurons like other macronutrients.

Previous studies have shown that alcohol can increase food intake through potentiating the rewarding properties of food (Yeomans, 2004; Yeomans et al., 1999) or increasing activity in AgRP neurons (Cains et al., 2017). In contrast, we observed short-term decreases and no long-term changes in food intake or body weight following alcohol administration in mice. The short-term decreases in food intake following alcohol are consistent with decreased AgRP neuron activity following alcohol. The discrepancy in the ability of alcohol to modulate food intake may be due to paradigm differences or the complex cognitive effects of alcohol on the control of food intake in humans. Based on the current results, reported increases in food intake in humans following alcohol are not likely due to changes in hypothalamic neuron activity.

Why is long-term food intake unaffected when AgRP neuron activity is decreased following alcohol administration? One potential explanation is that mice do not recognize the caloric content of alcohol. Indeed, existing evidence suggests that alcohol is not sensed as food (Poppitt et al., 1996; Tremblay et al., 1995), and thus the effects of alcohol on AgRP neurons may only reflect the "drug effect" of alcohol. This is supported by the inability of AgRP neuron stimulation to drive alcohol intake. An alternate explanation for the lack of effects of alcohol on energy balance involves its overall effect on brain network activity. For example, neural activity in anorexigenic POMC neurons, which is normally increased in satiety (Chen et al., 2015; Mandelblat-Cerf et al., 2015), is not affected by alcohol. Further, given the brain-wide activity changes seen following alcohol consumption (Bloom and Siggins, 1987; Chang et al., 1995; Ehlers et al., 2012; Thiele et al., 2000), other circuits not assessed in our study may cancel the anorexic effect of reduced AgRP neuron activity.

### *In Vivo* Neural Activity Monitoring

Our study highlights the importance of real-time, *in vivo* recordings in awake and behaving animals. We find that the effects of alcohol (using three different routes of administration) on AgRP neuron activity are opposite of previously observed results from *ex vivo* slice preparations (Cains et al., 2017). *In vivo* neural activity monitoring provides better temporal resolution compared to *ex vivo* techniques. For example, while it has previously been demonstrated that nicotine increases POMC neuron activity (Mineur et al., 2011), our results reveal that nicotine first causes a dramatic and acute (~10 min) reduction in both AgRP and POMC neuron activity. In comparison to alcohol, activity changes in response to nicotine recover on a faster time course. In fact, POMC neuron activity appears to be elevated following this recovery (10–25 min post-injection), similar to previous findings (Mineur et al., 2011). The increased temporal resolution gained by monitoring neural circuits in real time, combined with the ability to understand brain integration of peripheral signals in the behaving animal, highlights the importance of *in vivo* neural activity assessment. Further, monitoring calcium dynamics is a reasonable proxy for neuron firing rates, as previous work has demonstrated a relationship between action potentials and calcium-dependent fluorescence (Akerboom et al., 2012), particularly in AgRP neurons (Betley et al., 2015). Ultimately, our findings suggest that real-time *in vivo* neural activity monitoring is necessary to substantiate and confirm detailed *in vitro* electrophysiological analyses. Taken together, such studies enable a comprehensive understanding of neural circuit mechanisms that control behavior.

### Multiple Pathways Mediate Control of Homeostatic Neural Circuits

Our findings reveal the existence of vagal and non-vagal modes of signaling for the regulation of neural activity in hypothalamic AgRP neurons. By combining *in vivo* neural activity recordings with a classical vagal lesioning technique, our data demonstrate that alcohol reduces AgRP neuron activity in a vagal-independent manner. This is contrasted by the vagal-dependent effects of fat or satiation signals such as CCK or PYY on AgRP neuron activity. Many studies have suggested that the vagus nerve is required for the intake-suppressive effects of satiation signals

**Figure 7. AgRP Neuron Activity Potentiates Dopamine Signaling in Response to Food and Drugs**

(A) Schematic illustrating the expression of the excitatory DREADD hM3Dq in AgRP neurons and the dopamine (DA) sensor in the nucleus accumbens (NAc). Fiber photometry was used to monitor dopamine signaling in the NAc while manipulating AgRP neuron activity with the DREADD ligand clozapine N-oxide (CNO).

(B) Experimental timelines: saline or CNO was injected 30 min prior to food or drug delivery, and NAc dopamine signaling was monitored.

(C) Food (chow) intake in *ad libitum*-fed mice expressing hM3Dq in AgRP neurons and DA sensor in the NAc 1 h following i.p. injection of saline or CNO (2.5 mg/kg) (n = 7/group, paired t test, $p < 0.001$).

(D) Average ΔF/F of DA sensor in *ad libitum*-fed mice pretreated with i.p. injections of saline or CNO during food (chow) presentation (n = 7/group). Signals are aligned to food presentation. Green, 490 nm signal. Darker lines represent means and lighter shaded areas represent SEMs.

(E) Maximum ΔF/F of the 490 nm signal of mice in (D) following food presentation (n = 7/group, paired t test, $p < 0.05$).

(F) Mean ΔF/F of the 490 nm signal of mice in (D) from 0 to 1 min following food presentation (n = 7/group, paired t test, $p < 0.001$).

(G) Average ΔF/F of DA sensor in *ad libitum*-fed mice pretreated with i.p. injections of saline or CNO during gastric infusion of 15% EtOH (n = 8/group).

(H) Heatmaps reporting ΔF/F of the 490 nm signal of the recordings in individual mice in (G).

(I) Mean ΔF/F of the 490 nm signal in 3 min bins during gastric infusion of the mice in (G) (n = 8/group, two-way repeated-measures ANOVA, $p < 0.05$).

(J) Average ΔF/F of DA sensor in *ad libitum*-fed mice pretreated with i.p. injections of saline or CNO during i.p. injection of nicotine (1.5 mg/kg) (n = 7/group).

(K) Heatmaps reporting ΔF/F of the 490 nm signal of the recordings in individual mice in (J).

(L) Mean ΔF/F of the 490 nm signal in 3 min bins from mice injected with nicotine in (J) (n = 7/group, two-way repeated-measures ANOVA, p = ns). Data are expressed as mean ± SEM, ns $p > 0.05$, t tests and post hoc comparisons: *$p < 0.05$, **$p < 0.01$, ***$p < 0.001$; ANOVA interaction: ∞ ∞ ∞ $p < 0.001$; ANOVA main effect of group: ☼☼$p < 0.01$, ☼☼☼$p < 0.001$. See also Figures S7 and S8.

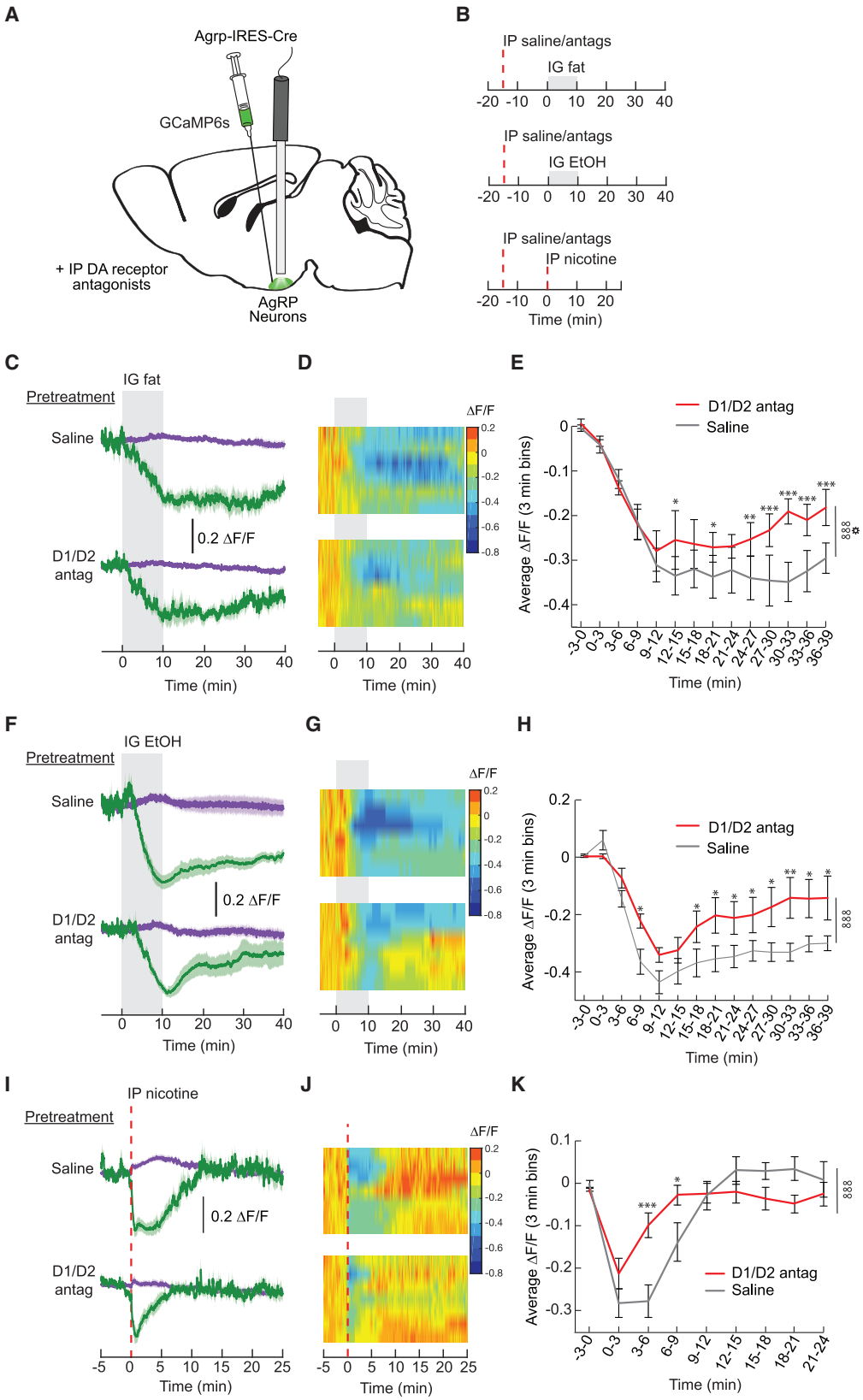


*(legend on next page)*

(Berthoud, 2008; Joyner et al., 1993; Schwartz and Moran, 1996), an effect that is mediated at least in part through hindbrain signaling (Grill and Hayes, 2012). Here, we have demonstrated that gut-brain vagal signaling is required for the effects of satiation signals on AgRP neuron activity, suggesting that the vagus nerve transmits signals to the hindbrain that are subsequently propagated to higher-order structures including the hypothalamus. The ability of satiation signals to influence hypothalamic neuron activity through vagal signaling resonates with recent data showing that CCK signals through the vagus nerve to increase dopamine signaling in the striatum (Han et al., 2018). Thus, both homeostatic and reward circuits receive gut signals through the vagus nerve. The mechanisms through which vagal afferents coordinate and distribute signals to downstream brain regions remain a compelling topic for future investigation.

How does alcohol modulate neural activity in a vagal-independent manner? It has been previously shown that alcohol acts directly on midbrain reward pathways to influence neural activity. We and others have shown that *in vivo* activity of dopaminergic neurons in the VTA is increased by alcohol in a dose-dependent manner (Gessa et al., 1985). This is thought to be mediated via a decrease in presynaptic GABAergic input onto DA neurons (Ostroumov et al., 2016; Stobbs et al., 2004) as well as direct excitatory action on DA neurons (Brodie et al., 1999; Koyama et al., 2007; Okamoto et al., 2006). Here, we found that alcohol reduced AgRP neuron activity following direct infusion into the lateral ventricle. These data suggest that alcohol acts directly in the brain to affect activity in hypothalamic neurons, in addition to dopamine circuits. Given that direct application of alcohol can increase *ex vivo* AgRP neuron activity (Cains et al., 2017), it is likely that circuit mechanisms lead to the reduction of AgRP neuron activity that we observed following peripheral or central alcohol administration. The precise circuit mechanisms that mediate these effects remain to be determined.

## Conclusion

Our findings reveal the ability of non-nutritive drugs to influence activity in homeostatic feeding circuits and demonstrate that multiple pathways exist to signal these neural populations. We have revealed a bidirectional, interdependent modulation of classical homeostatic and reward circuits that robustly influence behavior. By developing a mechanistic understanding of how nutritive and non-nutritive substances influence the activity of reinforcement circuits in the brain, these experiments provide novel targets for the development of weight loss and addiction therapies.

## STAR★METHODS

Detailed methods are provided in the online version of this paper and include the following:

- KEY RESOURCES TABLE
- LEAD CONTACT AND MATERIALS AVAILABILITY
- EXPERIMENTAL MODEL AND SUBJECT DETAILS
- METHOD DETAILS
  - Recombinant Adeno-Associated Virus (rAAV) Constructs and Production
  - Viral Injections and Fiber Optic/Cannula Implantation
  - Gastric Catheter Implantation
  - Complete Subdiaphragmatic Vagotomy
  - Food Restriction
  - Dual-wavelength Fiber Photometry
  - Fiber Photometry Data Analysis
  - Fiber Photometry Recordings During Food Intake
  - Fiber Photometry Recordings During Ethanol (EtOH), Fat, Glucose, or Drug Administration
  - Food Intake Experiments
  - *In Vivo* Photostimulation
  - Photostimulation-induced EtOH Intake
  - Photostimulation-induced glucose or glucose/quinine intake
  - Photostimulation induced glucose or glucose/EtOH intake
  - Effects of AgRP neuron activity on DA signaling
  - Effects of DA receptor antagonism on AgRP neuron activity
  - Histology, Immunohistochemistry, and Imaging
- QUANTIFICATION AND STATISTICAL ANALYSES

**Figure 8. Dopamine Receptor Antagonists Attenuate AgRP Neuron Responses to Nutrients and Drugs**

(A) Schematic for monitoring GCaMP6s dynamics in AgRP neurons using fiber photometry following i.p. injection of D1/D2 dopamine receptor antagonists (raclopride, 1 mg/kg; SCH 23390, 0.1 mg/kg).

(B) Experimental timelines: i.p. injections of saline or D1/D2 receptor antagonists were given 15 min prior to food or drug administration, and AgRP neuron activity was monitored.

(C) Average ΔF/F of GCaMP6s signal in AgRP neurons of food-deprived mice pretreated with i.p. injections of saline or D1/D2 antagonists during intragastric infusion of 1 kcal fat (n = 6/group). Signals are aligned to the start of the infusion. Green, 490 nm signal; purple, 405 nm control signal. Darker lines represent means, and lighter shaded areas represent SEMs.

(D) Heatmaps reporting ΔF/F of the 490 nm signal of the recordings in individual mice in (C).

(E) Mean ΔF/F of the 490 nm signal in 3 min bins during intragastric infusion of fat of the mice in (C) (n = 6/group, two-way repeated-measures ANOVA, $p < 0.001$).

(F) Average ΔF/F of GCaMP6s signal in AgRP neurons of food-deprived mice pretreated with i.p. injections of saline or D1/D2 antagonists during intragastric infusion of 15% EtOH (n = 6/group).

(G) Heatmaps reporting ΔF/F of the 490 nm signal of the recordings in individual mice in (F).

(H) Mean ΔF/F of the 490 nm signal in 3 min bins during intragastric infusion of EtOH of the mice in (F) (n = 6/group, two-way repeated-measures ANOVA, $p < 0.001$).

(I) Average ΔF/F of GCaMP6s signal in AgRP neurons of food-deprived mice pretreated with i.p. injections of saline or D1/D2 antagonists during i.p. injection of nicotine (1.5 mg/kg) (n = 7/group).

(J) Heatmaps reporting ΔF/F of the 490 nm signal of the recordings in individual mice in (I).

(K) Mean ΔF/F of the 490 nm signal in 3 min bins during i.p. injection of nicotine of the mice in (I) (n = 7/group, two-way repeated-measures ANOVA, $p < 0.001$). Data are expressed as mean ± SEM, ns $p > 0.05$, t tests and post hoc comparisons: *$p < 0.05$, **$p < 0.01$, ***$p < 0.001$; ANOVA interaction: ∞ ∞ ∞$p < 0.001$; ANOVA main effect of group: ☼$p < 0.05$. See also Figures S7 and S8.

## SUPPLEMENTAL INFORMATION

Supplemental Information can be found online at https://doi.org/10.1016/j.neuron.2019.05.050.

## ACKNOWLEDGMENTS

We thank Zhenwei Su, Jessica Naredo, Olivia Bruyn, and Frank Aguilar for experimental assistance; Gary Schwartz (and NIH P30DK26687, NY Obesity Research Center Animal Phenotyping Core) for technical and conceptual assistance with vagotomy experiments and for comments on the manuscript; Marc Fuccillo for assistance with reagents; Matthew Hayes and Harvey Grill for inspiration and advice on vagotomy experiments; and William Doyon for comments on the manuscript. This research was funded by the University of Pennsylvania School of Arts and Sciences (to J.N.B.), the American Heart Association (17SDG33400158 to J.N.B.), the American Diabetes Association (to J.N.B), L'Oréal USA (to A.L.A), The Obesity Society (to A.L.A.), and the NIH (1R01DK114104 to J.N.B, F32DK112561 to A.L.A., K99DK119574 to A.L.A., and T32NS105607 to N.G.).

## AUTHOR CONTRIBUTIONS

A.L.A. and J.N.B. initiated the project and prepared the manuscript with comments from all authors. A.L.A., N.G., M.L.K., O.P., A.V., and J.N.B. designed experiments, performed experiments, and/or analyzed data.

## DECLARATION OF INTERESTS

The authors declare no competing interests.

Received: November 21, 2018
Revised: April 6, 2019
Accepted: May 30, 2019
Published: July 2, 2019

## REFERENCES

Akerboom, J., Chen, T.W., Wardill, T.J., Tian, L., Marvin, J.S., Mutlu, S., Calderón, N.C., Esposti, F., Borghuis, B.G., Sun, X.R., et al. (2012). Optimization of a GCaMP calcium indicator for neural activity imaging. J. Neurosci. *32*, 13819–13840.

Alhadeff, A.L., Rupprecht, L.E., and Hayes, M.R. (2012). GLP-1 neurons in the nucleus of the solitary tract project directly to the ventral tegmental area and nucleus accumbens to control for food intake. Endocrinology *153*, 647–658.

Alhadeff, A.L., Su, Z., Hernandez, E., Klima, M.L., Phillips, S.Z., Holland, R.A., Guo, C., Hantman, A.W., De Jonghe, B.C., and Betley, J.N. (2018). A neural circuit for the suppression of pain by a competing need state. Cell *173*, 140–152.

Aponte, Y., Atasoy, D., and Sternson, S.M. (2011). AGRP neurons are sufficient to orchestrate feeding behavior rapidly and without training. Nat. Neurosci. *14*, 351–355.

Atasoy, D., Betley, J.N., Su, H.H., and Sternson, S.M. (2012). Deconstruction of a neural circuit for hunger. Nature *488*, 172–177.

Bäckman, C.M., Malik, N., Zhang, Y., Shan, L., Grinberg, A., Hoffer, B.J., Westphal, H., and Tomac, A.C. (2006). Characterization of a mouse strain expressing Cre recombinase from the 3′ untranslated region of the dopamine transporter locus. Genesis *44*, 383–390.

Balthasar, N., Coppari, R., McMinn, J., Liu, S.M., Lee, C.E., Tang, V., Kenny, C.D., McGovern, R.A., Chua, S.C., Jr., Elmquist, J.K., and Lowell, B.B. (2004). Leptin receptor signaling in POMC neurons is required for normal body weight homeostasis. Neuron *42*, 983–991.

Batterham, R.L., Cowley, M.A., Small, C.J., Herzog, H., Cohen, M.A., Dakin, C.L., Wren, A.M., Brynes, A.E., Low, M.J., Ghatei, M.A., et al. (2002). Gut hormone PYY(3-36) physiologically inhibits food intake. Nature *418*, 650–654.

Berthoud, H.R. (2008). Vagal and hormonal gut-brain communication: from satiation to satisfaction. Neurogastroenterol. Motil. *20* (*Suppl 1*), 64–72.

Betley, J.N., Cao, Z.F., Ritola, K.D., and Sternson, S.M. (2013). Parallel, redundant circuit organization for homeostatic control of feeding behavior. Cell *155*, 1337–1350.

Betley, J.N., Xu, S., Cao, Z.F.H., Gong, R., Magnus, C.J., Yu, Y., and Sternson, S.M. (2015). Neurons for hunger and thirst transmit a negative-valence teaching signal. Nature *521*, 180–185.

Beutler, L.R., Chen, Y., Ahn, J.S., Lin, Y.-C., Essner, R.A., and Knight, Z.A. (2017). Dynamics of gut-brain communication underlying hunger. Neuron *96*, 461–475.

Bhavsar, S., Watkins, J., and Young, A. (1998). Synergy between amylin and cholecystokinin for inhibition of food intake in mice. Physiol. Behav. *64*, 557–561.

Bloom, F.E., and Siggins, G.R. (1987). Electrophysiological action of ethanol at the cellular level. Alcohol *4*, 331–337.

Bouret, S.G., Draper, S.J., and Simerly, R.B. (2004). Formation of projection pathways from the arcuate nucleus of the hypothalamus to hypothalamic regions implicated in the neural control of feeding behavior in mice. J. Neurosci. *24*, 2797–2805.

Broberger, C., Johansen, J., Johansson, C., Schalling, M., and Hökfelt, T. (1998). The neuropeptide Y/agouti gene-related protein (AGRP) brain circuitry in normal, anorectic, and monosodium glutamate-treated mice. Proc. Natl. Acad. Sci. USA *95*, 15043–15048.

Brodie, M.S., and Dunwiddie, T.V. (1990). Cocaine effects in the ventral tegmental area: evidence for an indirect dopaminergic mechanism of action. Naunyn Schmiedebergs Arch. Pharmacol. *342*, 660–665.

Brodie, M.S., Pesold, C., and Appel, S.B. (1999). Ethanol directly excites dopaminergic ventral tegmental area reward neurons. Alcohol. Clin. Exp. Res. *23*, 1848–1852.

Cabeza de Vaca, S., and Carr, K.D. (1998). Food restriction enhances the central rewarding effect of abused drugs. J. Neurosci. *18*, 7502–7510.

Cains, S., Blomeley, C., Kollo, M., Rácz, R., and Burdakov, D. (2017). Agrp neuron activity is required for alcohol-induced overeating. Nat. Commun. *8*, 14014.

Calarco, C.A., and Picciotto, M.R. (2019). Nicotinic acetylcholine receptor signaling in the hypothalamus: mechanisms related to nicotine's effects on food intake. Nicotine Tob. Res. Published online January 25, 2019. https://doi.org/10.1093/ntr/ntz010.

Calarco, C.A., Li, Z., Taylor, S.R., Lee, S., Zhou, W., Friedman, J.M., Mineur, Y.S., Gotti, C., and Picciotto, M.R. (2018). Molecular and cellular characterization of nicotinic acetylcholine receptor subtypes in the arcuate nucleus of the mouse hypothalamus. Eur. J. Neurosci. *48*, 1600–1619.

Carr, K.D. (2002). Augmentation of drug reward by chronic food restriction: behavioral evidence and underlying mechanisms. Physiol. Behav. *76*, 353–364.

Cederbaum, A.I. (2012). Alcohol metabolism. Clin. Liver Dis. *16*, 667–685.

Chang, S.L., Patel, N.A., and Romero, A.A. (1995). Activation and desensitization of Fos immunoreactivity in the rat brain following ethanol administration. Brain Res. *679*, 89–98.

Chen, Y., Lin, Y.C., Kuo, T.W., and Knight, Z.A. (2015). Sensory detection of food rapidly modulates arcuate feeding circuits. Cell *160*, 829–841.

Cone, J.J., McCutcheon, J.E., and Roitman, M.F. (2014). Ghrelin acts as an interface between physiological state and phasic dopamine signaling. J. Neurosci. *34*, 4905–4913.

Dasen, J.S., Tice, B.C., Brenner-Morton, S., and Jessell, T.M. (2005). A Hox regulatory network establishes motor neuron pool identity and target-muscle connectivity. Cell *123*, 477–491.

Dossat, A.M., Lilly, N., Kay, K., and Williams, D.L. (2011). Glucagon-like peptide 1 receptors in nucleus accumbens affect food intake. J. Neurosci. *31*, 14453–14457.

Ehlers, C.L., Wills, D.N., and Havstad, J. (2012). Ethanol reduces the phase locking of neural activity in human and rodent brain. Brain Res. *1450*, 67–79.

Epstein, A.N. (1959). Suppression of eating and drinking by amphetamine and other drugs in normal and hyperphagic rats. J. Comp. Physiol. Psychol. *52*, 37–45.

Flood, J.F., Smith, G.E., and Morley, J.E. (1987). Modulation of memory processing by cholecystokinin: dependence on the vagus nerve. Science *236*, 832–834.

Fulton, S., Pissios, P., Manchon, R.P., Stiles, L., Frank, L., Pothos, E.N., Maratos-Flier, E., and Flier, J.S. (2006). Leptin regulation of the mesoaccumbens dopamine pathway. Neuron *51*, 811–822.

Geisler, S., Derst, C., Veh, R.W., and Zahm, D.S. (2007). Glutamatergic afferents of the ventral tegmental area in the rat. J. Neurosci. *27*, 5730–5743.

Gessa, G.L., Muntoni, F., Collu, M., Vargiu, L., and Mereu, G. (1985). Low doses of ethanol activate dopaminergic neurons in the ventral tegmental area. Brain Res. *348*, 201–203.

Gill, K., Amit, Z., and Smith, B.R. (1996). Alcohol as a food: a commentary on Richter. Physiol. Behav. *60*, 1485–1490.

Grill, H.J., and Hayes, M.R. (2012). Hindbrain neurons as an essential hub in the neuroanatomically distributed control of energy balance. Cell Metab. *16*, 296–309.

Grobe, C.L., and Spector, A.C. (2008). Constructing quality profiles for taste compounds in rats: a novel paradigm. Physiol. Behav. *95*, 413–424.

Gunaydin, L.A., Grosenick, L., Finkelstein, J.C., Kauvar, I.V., Fenno, L.E., Adhikari, A., Lammel, S., Mirzabekov, J.J., Airan, R.D., Zalocusky, K.A., et al. (2014). Natural neural projection dynamics underlying social behavior. Cell *157*, 1535–1551.

Han, W., Tellez, L.A., Niu, J., Medina, S., Ferreira, T.L., Zhang, X., Su, J., Tong, J., Schwartz, G.J., van den Pol, A., and de Araujo, I.E. (2016). Striatal dopamine links gastrointestinal rerouting to altered sweet appetite. Cell Metab. *23*, 103–112.

Han, W., Tellez, L.A., Perkins, M.H., Perez, I.O., Qu, T., Ferreira, J., Ferreira, T.L., Quinn, D., Liu, Z.W., Gao, X.B., et al. (2018). A neural circuit for gut-induced reward. Cell *175*, 887–888.

Hetherington, M.M., Cameron, F., Wallis, D.J., and Pirie, L.M. (2001). Stimulation of appetite by alcohol. Physiol. Behav. *74*, 283–289.

Hommel, J.D., Trinko, R., Sears, R.M., Georgescu, D., Liu, Z.W., Gao, X.B., Thurmon, J.J., Marinelli, M., and DiLeone, R.J. (2006). Leptin receptor signaling in midbrain dopamine neurons regulates feeding. Neuron *51*, 801–810.

Huang, H., Xu, Y., and van den Pol, A.N. (2011). Nicotine excites hypothalamic arcuate anorexigenic proopiomelanocortin neurons and orexigenic neuropeptide Y neurons: similarities and differences. J. Neurophysiol. *106*, 1191–1202.

Joyner, K., Smith, G.P., and Gibbs, J. (1993). Abdominal vagotomy decreases the satiating potency of CCK-8 in sham and real feeding. Am. J. Physiol. *264*, R912–R916.

Kenny, P.J. (2011). Reward mechanisms in obesity: new insights and future directions. Neuron *69*, 664–679.

Kopin, A.S., Mathes, W.F., McBride, E.W., Nguyen, M., Al-Haider, W., Schmitz, F., Bonner-Weir, S., Kanarek, R., and Beinborn, M. (1999). The cholecystokinin-A receptor mediates inhibition of food intake yet is not essential for the maintenance of body weight. J. Clin. Invest. *103*, 383–391.

Koyama, S., Brodie, M.S., and Appel, S.B. (2007). Ethanol inhibition of m-current and ethanol-induced direct excitation of ventral tegmental area dopamine neurons. J. Neurophysiol. *97*, 1977–1985.

Krashes, M.J., Koda, S., Ye, C., Rogan, S.C., Adams, A.C., Cusher, D.S., Maratos-Flier, E., Roth, B.L., and Lowell, B.B. (2011). Rapid, reversible activation of AgRP neurons drives feeding behavior in mice. J. Clin. Invest. *121*, 1424–1428.

Lapin, I.P., and Rogawski, M.A. (1995). Effects of D1 and D2 dopamine receptor antagonists and catecholamine depleting agents on the locomotor stimulation induced by dizocilpine in mice. Behav. Brain Res. *70*, 145–151.

Larkin, J.W., Binks, S.L., Li, Y., and Selvage, D. (2010). The role of oestradiol in sexually dimorphic hypothalamic-pituitary-adrena axis responses to intracerebroventricular ethanol administration in the rat. J. Neuroendocrinol. *22*, 24–32.

Lerner, T.N., Shilyansky, C., Davidson, T.J., Evans, K.E., Beier, K.T., Zalocusky, K.A., Crow, A.K., Malenka, R.C., Luo, L., Tomer, R., and Deisseroth, K. (2015). Intact-brain analyses reveal distinct information carried by SNc dopamine subcircuits. Cell *162*, 635–647.

Liu, S., and Borgland, S.L. (2015). Regulation of the mesolimbic dopamine circuit by feeding peptides. Neuroscience *289*, 19–42.

Luan, X., Sun, X., Guo, F., Zhang, D., Wang, C., Ma, L., and Xu, L. (2017). Lateral hypothalamic Orexin-A-ergic projections to the arcuate nucleus modulate gastric function in vivo. J. Neurochem. *143*, 697–707.

Madisen, L., Mao, T., Koch, H., Zhuo, J.M., Berenyi, A., Fujisawa, S., Hsu, Y.W., Garcia, A.J., 3rd, Gu, X., Zanella, S., et al. (2012). A toolbox of Cre-dependent optogenetic transgenic mice for light-induced activation and silencing. Nat. Neurosci. *15*, 793–802.

Mandelblat-Cerf, Y., Ramesh, R.N., Burgess, C.R., Patella, P., Yang, Z., Lowell, B.B., and Andermann, M.L. (2015). Arcuate hypothalamic AgRP and putative POMC neurons show opposite changes in spiking across multiple timescales. eLife *4*, e07122.

Mejías-Aponte, C.A., and Kiyatkin, E.A. (2012). Ventral tegmental area neurons are either excited or inhibited by cocaine's actions in the peripheral nervous system. Neuroscience *207*, 182–197.

Mineur, Y.S., Abizaid, A., Rao, Y., Salas, R., DiLeone, R.J., Gündisch, D., Diano, S., De Biasi, M., Horvath, T.L., Gao, X.B., and Picciotto, M.R. (2011). Nicotine decreases food intake through activation of POMC neurons. Science *332*, 1330–1332.

Mura, E., Taruno, A., Yagi, M., Yokota, K., and Hayashi, Y. (2018). Innate and acquired tolerance to bitter stimuli in mice. PLoS ONE *13*, e0210032.

Neary, N.M., Small, C.J., Druce, M.R., Park, A.J., Ellis, S.M., Semjonous, N.M., Dakin, C.L., Filipsson, K., Wang, F., Kent, A.S., et al. (2005). Peptide YY3-36 and glucagon-like peptide-17-36 inhibit food intake additively. Endocrinology *146*, 5120–5127.

Nieh, E.H., Matthews, G.A., Allsop, S.A., Presbrey, K.N., Leppla, C.A., Wichmann, R., Neve, R., Wildes, C.P., and Tye, K.M. (2015). Decoding neural circuits that control compulsive sucrose seeking. Cell *160*, 528–541.

Okamoto, T., Harnett, M.T., and Morikawa, H. (2006). Hyperpolarization-activated cation current (Ih) is an ethanol target in midbrain dopamine neurons of mice. J. Neurophysiol. *95*, 619–626.

Ostroumov, A., Thomas, A.M., Kimmey, B.A., Karsch, J.S., Doyon, W.M., and Dani, J.A. (2016). Stress increases ethanol self-administration via a shift toward excitatory GABA signaling in the ventral tegmental area. Neuron *92*, 493–504.

Poppitt, S.D., Eckhardt, J.W., McGonagle, J., Murgatroyd, P.R., and Prentice, A.M. (1996). Short-term effects of alcohol consumption on appetite and energy intake. Physiol. Behav. *60*, 1063–1070.

Powley, T.L., Fox, E.A., and Berthoud, H.R. (1987). Retrograde tracer technique for assessment of selective and total subdiaphragmatic vagotomies. Am. J. Physiol. *253*, R361–R370.

Raben, A., Agerholm-Larsen, L., Flint, A., Holst, J.J., and Astrup, A. (2003). Meals with similar energy densities but rich in protein, fat, carbohydrate, or alcohol have different effects on energy expenditure and substrate metabolism but not on appetite and energy intake. Am. J. Clin. Nutr. *77*, 91–100.

Richter, C.P. (1941). Alcohol as a food. Q. J. Stud. Alcohol *1*, 650–662.

Richter, C.P. (1953). Alcohol, beer and wine as foods. Q. J. Stud. Alcohol *14*, 525–539.

Rossi, M.A., and Stuber, G.D. (2018). Overlapping brain circuits for homeostatic and hedonic feeding. Cell Metab. *27*, 42–56.

Rothwell, N.J., and Stock, M.J. (1984). Influence of alcohol and sucrose consumption on energy balance and brown fat activity in the rat. Metabolism *33*, 768–771.

Saper, C.B., Chou, T.C., and Elmquist, J.K. (2002). The need to feed: homeostatic and hedonic control of eating. Neuron *36*, 199–211.

Schutz, Y. (2000). Role of substrate utilization and thermogenesis on body-weight control with particular reference to alcohol. Proc. Nutr. Soc. *59*, 511–517.

Schwartz, G.J., and Moran, T.H. (1996). Sub-diaphragmatic vagal afferent integration of meal-related gastrointestinal signals. Neurosci. Biobehav. Rev. *20*, 47–56.

Selvage, D. (2012). Roles of the locus coeruleus and adrenergic receptors in brain-mediated hypothalamic-pituitary-adrenal axis responses to intracerebroventricular alcohol. Alcohol. Clin. Exp. Res. *36*, 1084–1090.

Skibicka, K.P., Hansson, C., Alvarez-Crespo, M., Friberg, P.A., and Dickson, S.L. (2011). Ghrelin directly targets the ventral tegmental area to increase food motivation. Neuroscience *180*, 129–137.

Sternson, S.M., and Eiselt, A.K. (2017). Three pillars for the neural control of appetite. Annu. Rev. Physiol. *79*, 401–423.

Stobbs, S.H., Ohran, A.J., Lassen, M.B., Allison, D.W., Brown, J.E., and Steffensen, S.C. (2004). Ethanol suppression of ventral tegmental area GABA neuron electrical transmission involves N-methyl-D-aspartate receptors. J. Pharmacol. Exp. Ther. *311*, 282–289.

Stuber, G.D., and Wise, R.A. (2016). Lateral hypothalamic circuits for feeding and reward. Nat. Neurosci. *19*, 198–205.

Su, Z., Alhadeff, A.L., and Betley, J.N. (2017). Nutritive, post-ingestive signals are the primary regulators of AgRP neuron activity. Cell Rep. *21*, 2724–2736.

Sun, F., Zeng, J., Jing, M., Zhou, J., Feng, J., Owen, S.F., Luo, Y., Li, F., Wang, H., Yamaguchi, T., et al. (2018). A genetically encoded fluorescent sensor enables rapid and specific detection of dopamine in flies, fish, and mice. Cell *174*, 481–496.

Suter, P.M., Jéquier, E., and Schutz, Y. (1994). Effect of ethanol on energy expenditure. Am. J. Physiol. *266*, R1204–R1212.

Szczypka, M.S., Mandel, R.J., Donahue, B.A., Snyder, R.O., Leff, S.E., and Palmiter, R.D. (1999). Viral gene delivery selectively restores feeding and prevents lethality of dopamine-deficient mice. Neuron *22*, 167–178.

Thiele, T.E., Cubero, I., van Dijk, G., Mediavilla, C., and Bernstein, I.L. (2000). Ethanol-induced c-fos expression in catecholamine- and neuropeptide Y-producing neurons in rat brainstem. Alcohol. Clin. Exp. Res. *24*, 802–809.

Tong, Q., Ye, C.P., Jones, J.E., Elmquist, J.K., and Lowell, B.B. (2008). Synaptic release of GABA by AgRP neurons is required for normal regulation of energy balance. Nat. Neurosci. *11*, 998–1000.

Tremblay, A., Buemann, B., Thériault, G., and Bouchard, C. (1995). Body fatness in active individuals reporting low lipid and alcohol intake. Eur. J. Clin. Nutr. *49*, 824–831.

Volkow, N.D., and Wise, R.A. (2005). How can drug addiction help us understand obesity? Nat. Neurosci. *8*, 555–560.

Volkow, N.D., Wise, R.A., and Baler, R. (2017). The dopamine motive system: implications for drug and food addiction. Nat. Rev. Neurosci. *18*, 741–752.

Weststrate, J.A., Wunnink, I., Deurenberg, P., and Hautvast, J.G. (1990). Alcohol and its acute effects on resting metabolic rate and diet-induced thermogenesis. Br. J. Nutr. *64*, 413–425.

Wise, R.A., Spindler, J., deWit, H., and Gerberg, G.J. (1978). Neuroleptic-induced "anhedonia" in rats: pimozide blocks reward quality of food. Science *201*, 262–264.

Yeomans, M.R. (2004). Effects of alcohol on food and energy intake in human subjects: evidence for passive and active over-consumption of energy. Br. J. Nutr. *92* (*Suppl 1*), S31–S34.

Yeomans, M.R., Hails, N.J., and Nesic, J.S. (1999). Alcohol and the appetizer effect. Behav. Pharmacol. *10*, 151–161.

Yu, X., Li, W., Ma, Y., Tossell, K., Harris, J.J., Harding, E.C., Ba, W., Miracca, G., Wang, D., Li, L., et al. (2019). GABA and glutamate neurons in the VTA regulate sleep and wakefulness. Nat. Neurosci. *22*, 106–119.

Zalocusky, K.A., Ramakrishnan, C., Lerner, T.N., Davidson, T.J., Knutson, B., and Deisseroth, K. (2016). Nucleus accumbens D2R cells signal prior outcomes and control risky decision-making. Nature *531*, 642–646.

Zhou, Q.Y., and Palmiter, R.D. (1995). Dopamine-deficient mice are severely hypoactive, adipsic, and aphagic. Cell *83*, 1197–1209.

## STAR★METHODS

### KEY RESOURCES TABLE

| REAGENT or RESOURCE | SOURCE | IDENTIFIER |
|---|---|---|
| Antibodies | | |
| Guinea Pig Anti Islet | T. Jessell Lab | Dasen et al., 2005 |
| c-Fos (9F6) Rabbit mAb | Cell Signaling Technology | 22505, RRID AB_2247211 |
| Alexa Fluor 488 AffiniPure Donkey Anti-Rabbit IgG (H+L) | Jackson ImmunoResearch | 711-545-152. RRID AB_2313584 |
| Cy3 AffiniPure Donkey Anti-Guinea Pig IgG (H+L) | Jackson ImmunoResearch | 706-165-148 RRID AB_2340460 |
| Bacterial and Virus Strains | | |
| AAV1-Syn-Flex-GCaMP6s-WPRE-SV40 | University of Pennsylvania Vector Core | AV-1-PV2821 |
| AAV1-Syn-Flex-GCaMP6f-WPRE-SV40 | University of Pennsylvania Vector Core | AV-1-PV2819 |
| AAV5-hSyn-DIO-hM3D(Gq)-mCherry | Addgene | 44361-AAV5 |
| AAV9-hSyn-DA4.2 | Vigene | h-D01 |
| Chemicals, Peptides, and Recombinant Proteins | | |
| Dulbecco's phosphate-buffered saline | HyClone | SH30013.04 |
| Paraformaldehyde | MP Biomedicals | 150146 |
| Acrylamide 40% solution | Hoefer | GR400-500 |
| [2,2′-Azobis (2-imidazolin-2-yl) propane] dihydrochloride | Wako Chemicals | VA-044 |
| Sodium dodecyl sulfate | Sigma | L3771-100G |
| Isoflurane | Clipper | 0010250 |
| Meloxicam | Norbrook Laboratories | 55529-040-11 |
| Bupivacaine | Moore Medical | 52683 |
| Hydrogen peroxide | Ricca Chemical Company | R3821310-1BV |
| Fluoro-Gold | Fluorochrome | https://fluorochrome.com |
| Sodium chloride (NaCl) | Sigma-Aldrich | S7653-250G |
| Sterile saline | Pfizer | 00409-4888-12 |
| Caffeine | Sigma-Aldrich | C0750-100G |
| Cocaine hydrochloride | Sigma-Aldrich | C5776 |
| D-Amphetamine hemisulfate salt | Sigma-Aldrich | A5880 |
| Nicotine hydrogen tartrate salt | Glentham Life Sciences | GL9693 |
| Ethanol | Decon Laboratories | 2716 |
| Intralipid | Fresenius Kabi | NDC 0338-0519-13 |
| D-glucose | Sigma-Aldrich | G8270-100G |
| Saccharin | Thermo Fisher Scientific | AC149005000 |
| Ensure Plus, Vanilla | Abbott | 53642 |
| Quinine | Sigma-Aldrich | Q1125-5G |
| Clozapine-N-Oxide | Tocris | 4936 |
| Raclopride | Tocris | 1810 |
| SCH-23390 | Tocris | 0925 |
| Experimental Models: Organisms/Strains | | |
| Mouse: Agrp-IRES-Cre, $Agrp^{tm1(cre)Lowl}/J$ | The Jackson Laboratory | 012899 RRID IMSR_JAX:012899 |
| Mouse: Pomc-Cre, $POMC^{tg(Pomc1-Cre)16Lowl}/J$ | The Jackson Laboratory | 005965 RRID IMSR_JAX:005965 |

(*Continued on next page*)

| Continued | | |
|---|---|---|
| REAGENT or RESOURCE | SOURCE | IDENTIFIER |
| Mouse: DAT-IRES-Cre, B6.SJL-Slc6a3$^{tm1.1(cre)Bkmn}$/J | The Jackson Laboratory | 006660<br>RRID IMSR_JAX:006660 |
| Mouse: Ai32, B6;129S-*Gt(ROSA)26Sor*$^{tm32(CAG-COP4*H134R/EYFP)Hze}$/J | The Jackson Laboratory | 012569<br>RRID IMSR_JAX:012569 |
| Mouse: C57BL/6J | The Jackson Laboratory | 000664<br>RRID IMSR_JAX:000664 |
| Software and Algorithms | | |
| SigmaPlot | Systat Software | |
| MATLAB R2016a | MathWorks | https://www.mathworks.com/product/matlab.html |
| Synapse | Tucker-Davis Technologies | http://www.tdt.com/Synapse/index.html |
| ANY-maze | Stoelting | http://www.anymaze.co.uk |
| Other | | |
| Microliter syringe pump, PHD Ultra | Harvard Apparatus | 703007 |
| Optic fibers for fiber photometry | Doric | MF2.5, 400/430-0.48 |
| 405 nm LED | ThorLabs | M405F1 |
| 490 nm LED | ThorLabs | M470F3 |
| Amplifier | Tucker-Davis Technology | RZ5P |
| Femtowatt photoreceiver | Newport | 2151 |
| Optogenetic fiber | ThorLabs | FT200UMT |
| 1.25 mm zirconia ferrules | Kientech | FZI-LC-230 |
| Metabond | Parkell | S380 |
| Ortho-jet BCA Liquid | Lang Dental Manufacturing | B1306 |
| Jet Tooth Shade Powder | Lang Dental Manufacturing | 143069 |
| Micro-Renathane Tubing | Braintree Scientific | MRE033 |
| Guide cannulae | Plastics One | 8IC315GS5SPC |
| Internal cannulae | Plastics One | 8IC315IS5SPC |
| Dummy cannulae | Plastics One | 8IC315DCSXXC |

## LEAD CONTACT AND MATERIALS AVAILABILITY

Further information and requests for resources and reagents should be directed to and will be fulfilled by the Lead Contact, J. Nicholas Betley. (jnbetley@sas.upenn.edu).

## EXPERIMENTAL MODEL AND SUBJECT DETAILS

Mice were group housed on a 12-h light/12-h dark cycle with *ad libitum* access to food (Purina Rodent Chow, 5001) and water unless otherwise noted. Adult male and female mice (at least 8 weeks old) were used for experimentation. Agrp-IRES-Cre (*Agrp*$^{tm1(cre)Lowl}$/J) (Tong et al., 2008), Pomc-Cre (POMC$^{tg(Pomc1-Cre)16Lowl}$/J) (Balthasar et al., 2004), DAT-IRES-Cre (B6.SJL-*Slc6a3*$^{tm1.1(cre)Bkmn}$/J) (Bäckman et al., 2006), Ai32 (*B6;129S-Gt(ROSA)26Sor*$^{tm32(CAG-COP4*H134R/EYFP)Hze}$/J) (Madisen et al., 2012), and C57BL/6J mice were used for experimentation. All mice were habituated to handling and experimental conditions prior to experiments. For within-subject behavioral analyses, mice received all experimental conditions. For between-subject analyses, mice were randomly assigned to experimental conditions. We performed experiments in both male and female subjects, and did not observed any trends or significant sex differences. Thus, to ensure our studies were appropriately powered and to minimize the number of subjects who had to undergo surgical procedures, we combined males and females for analyses in all experiments. All procedures were approved by the University of Pennsylvania Institutional Animal Care and Use Committee.

## METHOD DETAILS

### Recombinant Adeno-Associated Virus (rAAV) Constructs and Production

The following Cre-dependent rAAV vectors were used: AAV1-Syn-Flex-GCaMP6s-WPRE-SV40 (titer: 4.216e13 GC/mL), AAV1-Syn-Flex-GCaMP6f-WPRE-SV40 (titer: 2.54e13 GC/mL), AAV5-hSyn-DIO-hM3Dq-mCherry (titer:1.3e13 GC/mL) and AAV9-hSyn-DA4.2

(titer 2.72e13 GC/mL). Viruses were produced by the University of Pennsylvania Vector Core, Addgene, or Vigene Biosciences. CAG, promoter containing a cytomegalovirus enhancer; the promoter, first exon and first intron of the chicken beta actin gene; and the splice acceptor of rabbit beta-globin gene. hSyn, human Synapsin 1 promoter. SV40, sequence motif promoting polyadenylation and termination. Flex, Cre-dependent flip-excision switch. WPRE, woodchuck hepatitis virus response element. GCaMP, Genetically encoded calcium indicator resulting from a fusion of GFP, M13 and Calmodulin. DIO, double-floxed inverted orientation. hM3Dq, human M3 muscarinic receptor.

### Viral Injections and Fiber Optic/Cannula Implantation

Mice were anesthetized with isoflurane (1.5%–3%, Clipper, 0010250) and pretreated with subcutaneous injections of meloxicam (5 mg/kg, Norbrook Laboratories, 55529-040-11) and bupivacaine (2 mg/kg, Moore Medical, 52683). Mice were placed into a stereotaxic apparatus (Stoelting, 51725D) and viral injections were performed as previously described (Alhadeff et al., 2018; Su et al., 2017). For fiber photometry (FP) experiments, unilateral injections of a virus designed to express GCaMP6s (for AgRP and POMC neurons), GcaMP6f (for DAT neurons), or DA sensor (DA4.2) (Sun et al., 2018) were performed in the arcuate hypothalamic nucleus (ARC, 300 μL total), ventral tegmental area (VTA, 300 μL total), or nucleus accumbens (NAc, 200 μL total), respectively, according to the following coordinates: ARC: bregma −1.35 mm, midline ± 0.25 mm, and skull −6.15-6.3 mm; VTA: bregma −3.2 mm, midline ± 1.2 mm, and skull −4.4 mm, at a 10° angle from vertical in the lateral to medial direction; NAc: bregma +1.0 mm, midline ± 1.2 mm, and skull −4.1-4.2 mm. A ferrule-capped optical fiber (400-μm core, NA 0.48, Doric, MF2.5, 400/430-0.48) was implanted 0.2 mm above the injection site and secured to the skull with Metabond cement (Parkell, S380) and dental cement (Lang Dental Manufacturing, Ortho-jet BCA Liquid, B1306 and Jet Tooth Shade Powder, 143069). For optogenetic activation of AgRP neurons, *Agrp*-IRES-Cre mice were crossed with Ai32 mice to express ChR2 in AgRP neurons. A unilateral optical fiber (200-μm core, NA 0.37, ThorLabs, FT200UMT) in a fiber ferrule (Kientech, FZI-LC-230) was placed over the ARC at bregma −1.35 mm, midline ± 0.25 mm, skull surface −5.8 mm. For chemogenetic activation of AgRP neurons, *Agrp*-IRES-Cre mice were bilaterally injected with a virus designed to express the excitatory designer receptor exclusively activated by designer drug (DREADD), hM3Dq. For central infusions, mice were implanted with a fiber photometry implant as described above, in addition to a unilateral 26-gauge guide cannulae (Plastics One, Roanoke, VA) in the lateral ventricle at bregma +0.7 mm, midline ± 1.0 mm, and skull surface −2.5 mm, at a 25° angle from vertical in the anterior to posterior direction. The cannula was secured to the skull with bone screws and dental cement. All mice were given at least 1 week for recovery before experiments were performed. *Post hoc* histology was used to confirm expression of GcaMP6 or ChR2 and proper placement of fibers and cannulae.

### Gastric Catheter Implantation

Mice were anesthetized with isoflurane (1.5%–3%) and treated with subcutaneous meloxicam (5 mg/kg), bupivacaine (2 mg/kg) and buprenorphine SR (1 mg/kg) analgesia. An abdominal midline incision was made through skin and muscle. Micro-Renathane catheter tubing (7-mm length, Braintree Scientific, MRE-033) with epoxy balls on each end (Devcon Clear Epoxy Adhesive, 92926, Lowes) was inserted into the fundus of the stomach through a puncture hole and secured with surgical mesh (5-mm diameter piece, Bard, 0112660). The other end of the catheter was directed out of an intrascapular incision. A metal cap was placed in the exposed end to seal the tubing. The gastric catheter was flushed with water after surgery to prevent blockage. Mice were fed with moistened chow and given at least 1 week for recovery prior to experimentation. Daily body weight was monitored until pre-surgical weight was regained.

### Complete Subdiaphragmatic Vagotomy

Mice were maintained on a liquid diet (Ensure Plus Vanilla, Abbott, 53642) for at least 3 days prior to surgery to promote survival and recovery. Mice were anesthetized with isoflurane (1.5%–3%) and treated with subcutaneous meloxicam (5 mg/kg), bupivacaine (2 mg/kg) and buprenorphine SR (1 mg/kg) analgesia. An abdominal midline incision was made through skin and muscle. The stomach was laporotomized to expose the esophagus, and the dorsal and ventral vagal trunks were then exposed by gently teasing them apart from the esophagus. The vagal trunks were resected and cauterized, and a gastric cannula was then implanted as described above. Control mice received a sham surgery that consisted of all surgical procedures except for the resection and cauterization of the vagus nerve. Functional verification of vagotomy was confirmed by examining CCK induced anorexia (see below). Histological verification of vagotomy was confirmed using an i.p. injection of 0.1% Fluoro-Gold and examining Fluoro-Gold presence in the dorsal motor nucleus of the vagus (DMX) 5 days post-injection.

### Food Restriction

For food restriction, mice were singly housed during experimentation and their food was restricted to maintain 85%–90% of their free-feeding body weight. Mice were weighed at the same time each day and given a chow aliquot (1.5-3.0 g) after experimentation to maintain their body weight. For 24-h food deprivation, mice were place in a new cage with clean bedding and water but no food 24 h prior to experimentation.

### Dual-wavelength Fiber Photometry

Dual-wavelength FP was performed as we and others have previously described (Lerner et al., 2015; Su et al., 2017; Zalocusky et al., 2016). Two excitation wavelengths were used: 490 and 405 nm. 490 nm excites calcium-dependent fluorescence from GCaMP6 protein, providing a measure of AgRP neuron activity. 405 nm excites calcium-independent fluorescence from GCaMP6 protein and serves as a control for movement and bleaching artifacts. Excitation light intensities were modulated at different frequencies (211 and 566 Hz for 490 and 405 nm, respectively) to avoid contamination from overhead lights (120 Hz and harmonics) and cross-talk between excitation lights. Excitation lights were generated through fiber-coupled LEDs (Thorlabs, M470F3 for 490 nm and M405F1 for 405 nm) and modulated by a real-time amplifier (Tucker-Davis Technology, RZ5P). Excitation lights were passed through bandpass filters (Thorlabs, MF469-35 for 490 nm and FB405-10 for 405 nm) before being collimated and combined by a 425-nm long-pass dichroic mirror (Thorlabs, DMLP425). The combined excitation light was sent into a patch cord made of a 400-μm core, NA 0.48, low-fluorescence optical fiber (Doric, MFP_400/430/1100-0.48_1.5_FCM-MF). The patch cord was connected to an implanted fiber contained in a 2.5-mm diameter ferrule via an interconnector (Thorlabs, ADAF2). GCaMP6 emission fluorescence signals were collected through the same patch cord, collimated, passed through a GFP emission filter (Thorlabs, MF525-39), and focused onto a femtowatt photoreceiver (Newport, Model 2151, gain set to AC LOW) using a lens (Edmund Optics, 62-561). The emission lights were converted to electrical signals, sampled at 1017 Hz, and demodulated by the RZ5P real-time processor. The FP experiments were controlled by Synapse software (Tucker-Davis Technology). Synchronized infra-red cameras (Ailipu Technology, ELP-USB100W05MT-DL36) controlled by Synapse were used to video-record mice during FP experiments.

Prior to experimentation, mice were habituated to experimental procedures. All FP experiments occurred in each individual's home cage with the lid removed. Baseline GCaMP6 fluorescence signals were set to similar levels by adjusting the output power of 490- and 405-nm LEDs. To achieve maximum sensitivity of signals, the 490-nm signal was set to occupy 50% of the detection range of the photoreceiver (20-100 μW at the tip of the fiber accounting for variations in GCaMP6 expressions and optical fiber positions over AgRP neurons). The 405-nm signal was set to occupy 5% of the detection range (2-10 μW output power at the tip of the fiber) to avoid saturating the detector. Baseline GCaMP6 fluorescence was recorded prior to a stimulus (5 min), and post-stimulus fluorescence was compared to baseline fluorescence as described below. Since POMC neuron GCaMP6s fluorescence (both calcium-dependent and calcium-independent) bleached modestly, we recorded neural activity for 25 min prior to the baseline recordings to minimize bleaching during experiments.

### Fiber Photometry Data Analysis

Demodulated data were exported from Synapse to MATLAB (MathWorks) using a script provided by Tucker-Davis Technology. The 490- and 405-nm signals were independently processed and normalized to baseline signals to determine ΔF/F, where $\Delta F/F = (F-F_{baseline})/F_{baseline}$ and $F_{baseline}$ is the median of pre-stimulus signal. No isosbestic normalization was introduced. Data were down-sampled to 1 Hz in MATLAB. The subsequent processing of FP data was performed in MATLAB and Excel. Mean ΔF/F was calculated by integrating ΔF/F over a period of time and then dividing by the integration time. Minimum and maximum ΔF/F were calculated by taking the averaged 10 s mean ΔF/F for each mouse at the average minimum or maximum of each recording.

### Fiber Photometry Recordings During Food Intake

At least 1 week following surgery, mice were food-restricted and screened for their neural response to chow refeeding. Baseline calcium activity was recorded for 5 min, and for 10 min following presentation of chow. Mice that had < 20% ΔF/F (AgRP neurons) or < 10% ΔF/F (POMC, DAT neurons or DA signal) were excluded from experiments. Further, to eliminate movement and bleaching artifacts and ensure that changes in ΔF/F were not due to a loose fiber connection, FP recordings with more than 15% change in the 405-nm signal were excluded from analyses.

### Fiber Photometry Recordings During Ethanol (EtOH), Fat, Glucose, or Drug Administration

#### *Effects of intragastric EtOH or fat on neural activity*

*Ad libitum* fed or food restricted mice were intragastrically infused with EtOH (0, 5, or 15% EtOH in water) or fat (10% intralipid or water) in a counterbalanced experimental design. Intragastric catheters were connected to tubing and a syringe placed into an infusion pump (Harvard Apparatus, 703007). 1 mL infusions were performed at a rate of 0.1 mL/min (Han et al., 2016; Su et al., 2017). FP recordings were performed for 35 min (5-min baseline recording and 30-min recording after start of infusion).

#### *Effects of EtOH drinking on neural activity*

Food restricted mice were given home cage access to 10% EtOH in 0.05% saccharin as well as 0.05% saccharin (control) in 2 bottles for 1 week. During testing, mice were presented with either EtOH or control solution and neural activity was recorded for 35 min (5-min baseline recording and 30-min recording after presentation of EtOH). EtOH and control solution intake was recorded at 5, 10, 15, and 30 min post-presentation. As a comparison, mice were given access to glucose (14%, equicaloric to 10% EtOH) in subsequent sessions and neural activity was monitored.

#### *Effects of lateral ventricle EtOH on neural activity*

Food restricted mice were given 1 μL lateral ventricle infusions of artificial cerebrospinal fluid (aCSF) or EtOH (0.8 μg), a dose/volume that does not cause neuronal damage (Larkin et al., 2010; Selvage, 2012) and was well-tolerated by our mice. Infusions were performed at 0.5 μL/min, and neural activity was recorded for 15 min (5-min baseline and 10 min post-start of infusion).

#### *Effects of drugs of abuse on neural activity*

Food restricted mice were given i.p. injection (10 μL/g) of saline, glucose (2 g/kg), caffeine (20 mg/kg), cocaine (10 mg/kg), amphetamine (1.5 mg/kg), or nicotine (1.5 mg/kg) and neural activity was recorded for 30 min (5-min baseline recording and 25-min post-injection). Drug doses were chosen based on the ability to condition a place preference.

### Food Intake Experiments

#### *Effects of IG EtOH on food intake*

*Ad libitum*-fed or food restricted mice were given IG infusion of EtOH (0, 5, or 15% in water) as described above. Food intake was recorded at 1, 2, 3, 4, and 24 h post-infusion.

#### *Effects of i.p. EtOH on food intake*

*Ad libitum*-fed or food restricted mice were given i.p. injections of EtOH (0 or 2 g/kg in saline) as described above. Food intake was recorded at 1, 2, 3, 4, and 24 h post-infusion.

#### *Effects of chronic EtOH on food intake and body weight*

*Ad libitum*-fed mice were given i.p. injections of EtOH (0 or 2 g/kg in saline) once daily for 2 weeks. Body weight and food intake were recorded each day immediately before i.p. injection.

#### *Effects of i.p. CCK on food intake*

Control or vagotomized mice were overnight food deprived and given i.p. injections of CCK (10 μg/kg in saline). Food intake was recorded for 30 min.

### *In Vivo* Photostimulation

Photostimulation of AgRP neurons was performed as previously described (Alhadeff et al., 2018), with 10-ms pulses at 20 Hz for 1 s, repeated every 4 s. The output beam from a diode laser (450 nm, Opto Engine) was controlled by a microcontroller (Arduino Uno) running a pulse generation script. The laser was coupled to a multimode optical fiber (200-μm core, NA 0.37, Doric) with a 1.25-mm OD zirconia ferrule (Kientech) and mating sleeve that allowed delivery of light to the brain by coupling to the implanted ferrule-capped optical fiber in the mouse. Power was set to ensure delivery of at least 2 $mW/mm^2$ to AgRP soma and was calculated using the following software: https://web.stanford.edu/group/dlab/cgi-bin/graph/chart.php.

### Photostimulation-induced EtOH Intake

Mice expressing ChR2 in AgRP neurons were habituated to experimental procedures. Mice were attached to patch fiber and lasers with access to either water, 10% EtOH, or 8% glucose in a counterbalanced experimental design. Water, EtOH, or glucose intake was recorded after a 1-h baseline, and again after 1 h of AgRP neuron stimulation. Data are displayed as AgRP-stimulated intake minus baseline intake.

### Photostimulation-induced glucose or glucose/quinine intake

To test if the aversive taste of EtOH may inhibit AgRP stimulation-induced intake, we measured the effect of AgRP neuron stimulation on glucose/quinine intake. Mice expressing ChR2 in AgRP neurons were habituated to experimental procedures. Mice were attached to patch fiber and lasers with access to either 8% glucose or 8% glucose with 0.3 mM quinine in a counterbalanced experimental design. This concentration of quinine reduces preference by approximately 50% in rats and mice (Grobe and Spector, 2008; Mura et al., 2018). Glucose and glucose/quinine intake were recorded after a 1-h baseline, and again after 1 h of AgRP neuron stimulation. Data are displayed as AgRP-stimulated intake minus baseline intake.

### Photostimulation induced glucose or glucose/EtOH intake

To further test whether mice detect the calories in EtOH, we examined AgRP stimulation-induced intake of glucose, or a glucose solution with added EtOH. Mice expressing ChR2 in AgRP neurons were habituated to experimental procedures. Mice were attached to patch fiber and lasers with access to either 4% glucose (0.16 kcal/mL) or 4% glucose/2.9% EtOH solution (0.32 kcal/mL, 0.16 kcal mL from glucose and 0.16 kcal/mL from EtOH) in a counterbalanced experimental design. Intake was recorded after a 1-h baseline, and again after 1 h of AgRP neuron stimulation. Data are displayed as AgRP-stimulated intake minus baseline intake.

### Effects of AgRP neuron activity on DA signaling

Food restricted mice expressing the excitatory DREADD, hM3Dq, in AgRP neurons and a DA sensor in the NAc were habituated to experimental procedures. The ligand for hM3Dq, clozapine-N-oxide (CNO, 2.5 mg/kg), was administered i.p. 30 min before mice were given chow, IG EtOH (15%), or i.p. nicotine (1.5 mg/kg) (or associated controls) and DA signaling was monitored for 10 min (chow), 45 min (EtOH) or 30 min (nicotine).

### Effects of DA receptor antagonism on AgRP neuron activity

Food restricted mice with GCaMP6s in AgRP neurons were habituated to experimental procedures. DA receptor antagonists (raclopride, 1 mg/kg and SCH-23390, 0.1 mg/kg (Lapin and Rogawski, 1995)) were administered 15 min before IG infusion of fat (1 kcal) or EtOH (15%) or i.p. injection of nicotine (1.5 mg/kg). AgRP neuron activity was monitored for 45 min (fat and EtOH) or 30 min (nicotine).

### Histology, Immunohistochemistry, and Imaging

Mice were deeply anesthetized with isoflurane (Clipper, 0010250) and transcardially perfused with 0.1 M Dulbecco's phosphate-buffered saline (PBS, HyClone, SH30013.04) followed by 4% paraformaldehyde (MP Biomedicals, 150146). Brains were post-fixed in 4% paraformaldehyde at 4°C for 4-6 h before being transferred to PBS. 100-200-μm coronal sections were prepared in PBS with a vibrating blade microtome (Leica, VT1000S). Epifluorescence images of viral fluorescence, fiber placements, and cannula placements were taken on a stereoscope (Leica, M165FC) to verify accuracy.

#### *Fos expression in arcuate hypothalamic neurons after i.p. EtOH*

Habituated mice were i.p. injected with EtOH (2 g/kg) or saline. 2 h later, mice were transcardially perfused and brains processed as described above. Brain sections were incubated overnight in 4% (v/v) acrylamide and 0.25% (w/v) catalyst ([2,2′-Azobis (2-imidazolin-2-yl) propane] dihydrochloride), and then incubated again in the same solution for 2-3 h at 37°C. Sections were washed 6 times in PBS, treated with 8% sodium dodecyl sulfate for 2-3 h, and washed again 10 times with PBS. Brain sections were next incubated overnight at 4°C in primary antibody [rabbit anti-cFos (1: 1:3,000, Cell Signaling, 2250) and Guinea pig anti-islet1/2 [1:5000] (Dasen et al., 2005). Sections were washed 3 times and incubated with species appropriate and minimally cross-reactive fluorophore-conjugated secondary antibodies (1:500, Jackson ImmunoResearch) for 3 h at room temperature. Sections were washed twice with PBS and mounted and coverslipped with Fluorogel. Epifluorescence and confocal images were taken on a Leica SPE laser scanning microscope using a 20X, 0.75-NA objective for quantification of Fos immunoreactivity. We quantified Fos+ neurons in Islet+ expressing neurons, since Islet exclusively marks AgRP and POMC neurons in the arcuate nucleus (Betley et al., 2013).

## QUANTIFICATION AND STATISTICAL ANALYSES

Data were expressed as means ± SEMs in figures and text. Paired or unpaired two-tailed t tests were performed as appropriate. One-way, two-way, and repeated-measures ANOVA were used to make comparisons across more than two groups using SigmaPlot. Test, statistics, significance levels, and sample sizes for each experiment are listed in Tables S1 and S2. Ns $p > 0.05$, t tests and post hoc comparisons: *$p < 0.05$, **$p < 0.01$, ***$p < 0.001$; interaction: ∞$p < 0.05$, ∞∞$p < 0.01$, ∞∞∞$p < 0.001$; main effect (group, condition or drug): ☼<0.05, ☼☼$p < 0.01$, ☼☼☼$p < 0.001$.